

Distribution of this document is unlimited.

OTOLITH SHEAR AND THE VISUAL PERCEPTION OF FORCE  
DIRECTION: DISCREPANCIES AND A PROPOSED RESOLUTION

Manning J. Correia, W. Carroll Hixson, and Jorma I. Niven

Bureau of Medicine and Surgery  
Project MR005.13-6001  
Subtask 1            Report No. 126

NASA Order R-93

Approved by

Captain Ashton Graybiel, MC USN  
Director of Research

Released by

Captain H. C. Hunley, MC USN  
Commanding Officer

1 December 1965

\*This study was supported in part by the Office of Advanced Research and Technology, National Aeronautics and Space Administration.

U. S. NAVAL AEROSPACE MEDICAL INSTITUTE  
U. S. NAVAL AVIATION MEDICAL CENTER  
PENSACOLA, FLORIDA

## SUMMARY PAGE

### THE PROBLEM

To analyse quantitatively the relationships between the magnitude and direction parameters of a static linear acceleration field, acting in either the sagittal or frontal head plane, and the visual perception of direction keyed to force as well as egocentric references.

### FINDINGS

The visual perception of the orientation of a force field, although found to be dependent upon the magnitude as well as direction of the field, was not found to be a linear function of the shear-directed otolith stimulus; in addition, discontinuities in the form of different subjective response measures for identical magnitude shear stimuli were observed. From these observations, it was possible to synthesize a tangent equation expression which quantitatively predicted the subjective response measure which would exist in fields of both sub and supragravitational levels. This equation defines the subjective perception of the orientation of a force field as  $\arctan A \tan \phi$  where  $A$  is the relative weight of the otolith membrane and  $\phi$  its orientation relative to the force field. A rationale for this equation and generalizations relative to extra-terrestrial environments are discussed.

### ACKNOWLEDGEMENTS

The authors wish to acknowledge the efforts of Mr. J. Cloud in the fabrication and installation of the mechanical equipments; Mr. A. N. Dennis and Mr. C. A. Lowery, in the construction, calibration, and operation of the instrumentation system; Mr. A. Thomas in the operational and analytical elements of the study as well as his contributions as a volunteer subject; Mrs. A. Thomas in the typing of numerous drafts of this manuscript; and HMC J. R. Cannon, HM3 E. L. Poe, HM3 T. E. Schwerin, and HM2 L. Brady, Jr. in the operation of the centrifuge.

## TABLE OF CONTENTS

SUMMARY PAGE . . . . .	ii
INTRODUCTION . . . . .	1
EXPERIMENT I . . . . .	2
Procedure	2
Results and Discussion	7
EXPERIMENT II . . . . .	17
Procedure	17
Results and Discussion	20
GENERAL DISCUSSION . . . . .	26
THE VALIDITY OF A LINEAR SINE EQUATION FOR THE PREDICTION OF OTOLITH-RELATED RESPONSES	26
Sagittal Plane Stimulus-Subjective Horizon Response	27
Frontal Plane Stimulus-Subjective Vertical/Ocular Counterroll Responses	34
A TANGENT EQUATION FOR THE PREDICTION OF OTOLITH-RELATED RESPONSES	39
REFERENCES . . . . .	46
APPENDIX A	
Experimental Data	Tables A1-A7
APPENDIX B	
Statistical Analyses	Tables B1-B7
APPENDIX C	
Description of Experimental Apparatus	

## INTRODUCTION

Man's responses to the myriads of environmental force fields which he encounters in the course of his normal activities are not ordinarily of pressing concern. That is not to say, however, that it is not of importance to define their relationships to the acceleration stimuli acting upon the man. Certainly there exists evidence from various terrestrially-oriented activities, notably aircraft operations, that a comprehensive and accurate understanding of the relevant sensory receptors and their mode of action is not only lacking but desirable. Vertigo or disorientation, while not a routine problem of every flight, can have serious implications for the success of the mission on which it does occur. In space operations likewise, although current experience has confirmed that disorientation is not a necessary concomitant of an orbital mission, one cannot dismiss lightly the potential costs of future occurrences.

Much information concerning the static orientation of an individual to linear force fields is available, some of it descriptive and qualitative in nature, some of it quantitative. Typically, this information derives from studies utilizing subjective judgments of the morphological orientation of a force field either during simple tilting in the normal gravitational field or during exposure to the resultant of centripetal and gravitational accelerations on various rotating devices. While it has been recognized that such judgments may be influenced by the magnitude as well as by the direction parameters of the field, only a few studies have been concerned primarily with establishing separate experimental control of these parameters, e.g., Schöne (9) who studied magnitude and direction effects of frontal and sagittal plane stimuli on subjective vertical and subjective horizon judgments, respectively; Colenbrander (1) who studied the effects of frontal plane stimuli on the subjective perception of vertical; and Miller and Graybiel (7) who studied the effects of frontal plane stimulation on the subjective perception of horizontal.

Only Schöne, however, and he for his horizon data only, attempted to formulate a predictive equation relating the subjective response to the stimulus. He stated that the subjective perception of horizon could be predicted as a direct linear function of a shear-directed force component acting along the plane of the sensory epithelium of the utricle.

The present study undertakes to differentiate quantitatively between the effects of magnitude and of direction varied independently and to correlate the findings for stimulation in the frontal and sagittal planes. The data are evaluated in terms of Schöne's model, the significance of certain discrepancies discussed, and an alternative predictive equation for perception of the horizon as well as one for estimates of subjective vertical presented.



## EXPERIMENT I

### PROCEDURE

#### Subjects

In this experiment four men served as subjects. Two of the subjects (MJC and JIN) were aware of the possible outcomes of the experiment. The other two subjects (DCA and AT) were naive with respect to the experimental objectives although prior to the test trials both had been practiced in making judgments and operating the visual target equipment.

#### Apparatus

The primary apparatus of both this experiment and Experiment II was the Pensacola Centrifuge-Slow Rotation Room I Facility and its related bioinstrumentation (3). The experimental conditions of the experiment were achieved by seating the subjects in a variable attitude chair fixed to the floor of a free-swinging cradle assembly which was bearing-supported at the end of the 20-foot radius centrifuge arm. During rotation the entire cradle assembly including the subject-chair moved radially outboard to the angle defined by the resultant of the centripetal and gravitational accelerations. As such, the resultant linear acceleration was always directed along an axis essentially at right angles to the floor of the cradle. Thus linear acceleration of variable magnitude and fixed morphological orientation could be presented to a subject during rotation of the centrifuge at constant angular velocity by preselecting different steady-state velocity levels. Experimental control of the direction of the resultant linear acceleration stimulus was afforded by the variable attitude chair. This chair permitted the subject to be tilted about the cradle bearing axis so that his head could be directed either radially inboard or radially outboard.

Photographs of the variable attitude chair installed on the free-swinging cradle, attached at the end of the radial arm of the centrifuge are presented in Figure 1. The subject-chair proper was attached to a circular gear ring which could be manually rotated in a plane normal to the vertical axis of the chair so that the subject could be seated radially with his face directed inboard or seated tangentially with his back in the direction of the counterclockwise centrifuge rotation as illustrated at the top and bottom, respectively, of Figure 1.

The circular gear ring was bearing supported at its extremities so that it could be manually tilted either inboard or outboard about an axis parallel to the floor of the cradle. This action allowed the vertical axis of the subject to be aligned exactly with an axis perpendicular to the floor of the cradle or to be tilted 15, 30, or 45 degrees to either side of this cradle axis. The orientation and tilt angle adjustments of the chair are illustrated in the photographs presented in Figure 2.

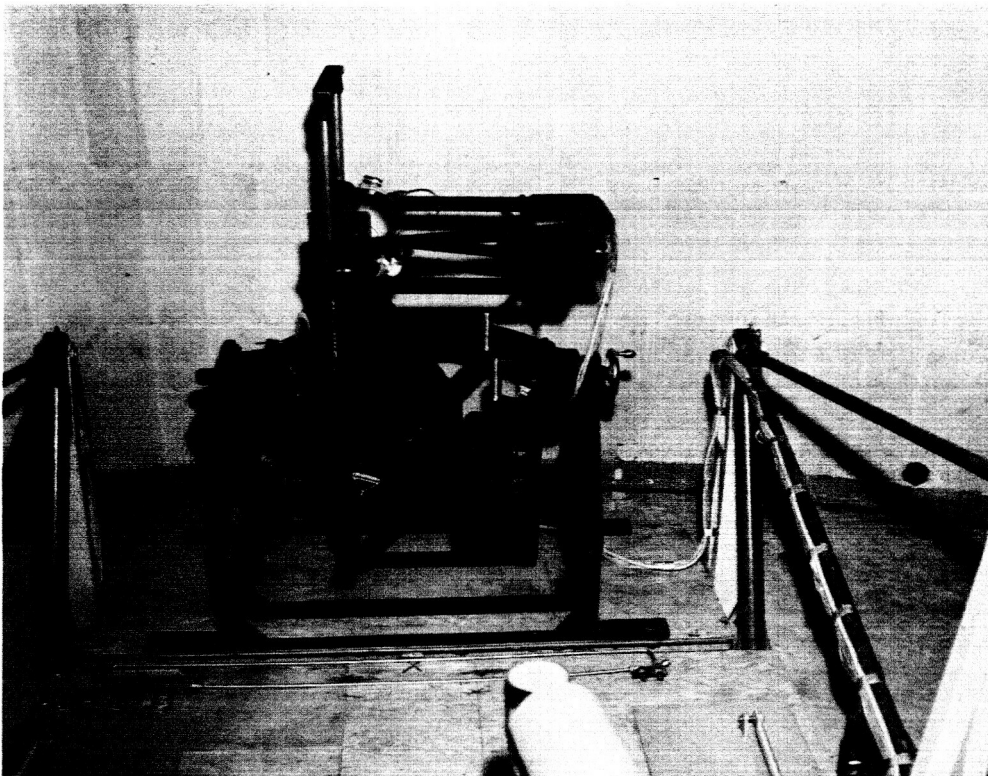
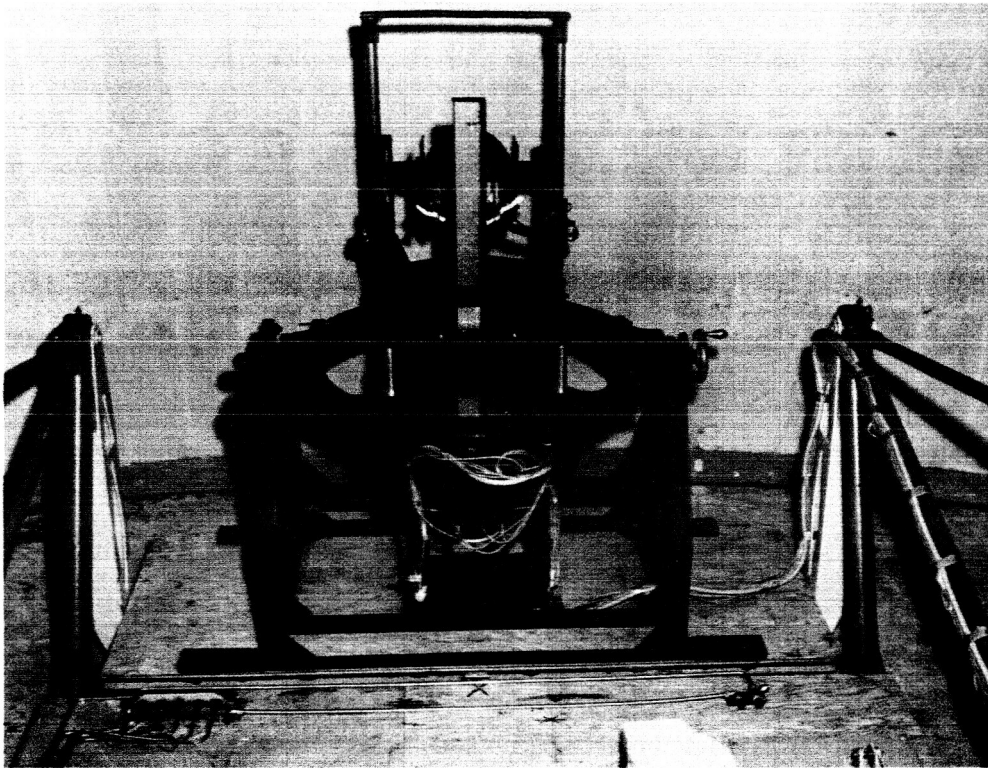


Figure 1

Variable attitude chair shown positioned radially (top) and tangentially (bottom) on the free-swinging cradle assembly pivoted at the end of the centrifuge arm.

With free-swinging cradle assemblies of the type discussed herein, serious errors can arise in the direction or orientation of the linear acceleration as a result of such factors as the finite length of the cradle arm, the relative displacement of the subject's head from the cradle axis, and cradle unbalance due to the mass distribution of experimental equipment installed aboard the cradle. These factors when acting in combination can result in significant stimulus direction errors which can easily be in the  $\pm 5$ - to  $\pm 7$ -degree range. To minimize these errors a calibration procedure was developed to ensure accurate experimental control of the magnitude and direction of the stimuli acting at head level of the subject. A triaxial accelerometer module with three orthogonally mounted force-balance type linear accelerometers was installed on the subject-chair at head level. The module was oriented so that the output of two accelerometers, as recorded by a digital voltmeter, could accurately establish both the magnitude and direction of the resultant of the gravitational and centripetal accelerations which existed for a given centrifuge velocity. Measurement of the latter was provided by a digital frequency meter which recorded pulse signals from a magnetic proximity sensor and ferrous gear assembly attached to the centrifuge proper and provided a readout of angular velocity to within  $\pm 0.02$  RPM in a ten-second counting period. With this apparatus, and a dummy load placed in the subject-chair, it was possible to measure the magnitude and direction of the stimulus for all combinations of chair orientation, chair tilt angle, and resultant acceleration magnitude level. Deviations of the actual from the desired stimulus were compensated for by lead counterbalances of variable weight and position. By counterbalancing for an average load in each stimulus configuration, directional errors of the resultant acceleration were reduced to within  $\pm 2$  degrees of the desired morphological orientation.

As may be seen in Figure 2, the subject's head was immobilized by means of a modified Navy APH-5 helmet which was rigidly fixed to the back of the chair; head constraint to the helmet was established by custom-fitted liners and a compression type chin strap. The body was held fixed by means of a combination shoulder-waist harness strap assembly. Headsets integral to the helmet and a lip microphone enabled the subject to remain in voice communication during the experimental trials.

In this experiment two different types of visual targets, the technical details of which are described in Appendix C, were used. When the subject was seated radially, his task was to align a horizontal luminous rod, 7 inches long and 1/16th inch wide, to his perception of the horizon (see Figures 2 and C 3 ). The vertical displacement of this target could be controlled either by the subject or the experimenter and its position recorded within  $\pm 0.05$  inch. As illustrated in the top photograph of Figure 2, the linear target assembly was positioned relative to the subject so that the target rod, horizontally oriented as viewed by the subject, could be elevated up to 15 inches above or depressed to 15 inches below mean eye level. When the subject was seated tangentially, his task was to set an angular displacement target to his perception of vertical. The target rod was identical to that described for the linear displacement target. The angular displacement of the target rod could be controlled by either the

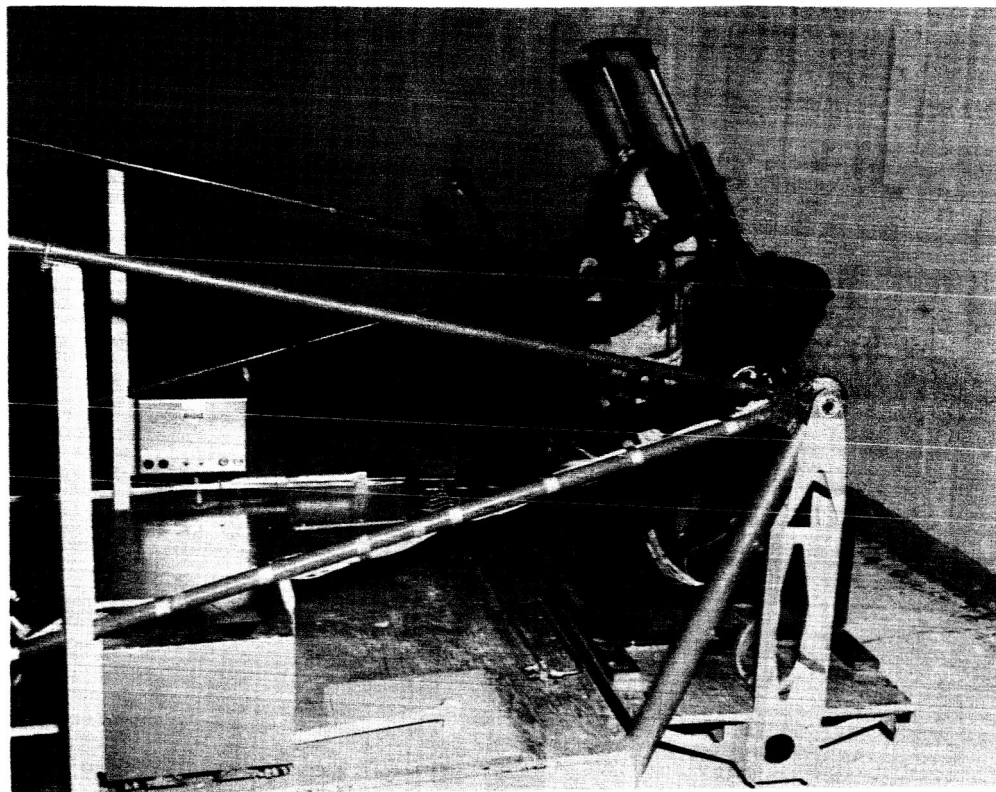


Figure 2

Subject shown seated facing radially inboard with variable attitude chair tilted  $30^\circ$  inboard and centrifuge at rest to illustrate the  $|\bar{A}_{xz}| = 1.0 g$ ,  $\omega_y = -30^\circ$  stimulus condition (top). Subject shown seated tangentially with back in direction of rotation with variable attitude chair tilted  $30^\circ$  outboard and a  $48^\circ$  crotch angle to simulate the  $\bar{A}_{yz} = 1.5 g$ ,  $\omega_x = +30^\circ$  stimulus condition (bottom).

subject or experimenter and its position recorded within  $\pm 0.1$  degree. The target, located directly in front of the subject as shown in the bottom photograph, Figure 2, could be displaced over a full 360 degrees in either direction.

The visual targets were installed on an instrument shelf in front of the subject and supported by means of two vertical rods fixed to the sides of the chair. Compression type locks on these rods allowed the instrument shelf to be raised or lowered so that the center of the visual target could be positioned at eye level for each subject. Since the instrument shelf was fixed relative to the subject-chair, the orientation of the visual target housing relative to the eyes of the subject remained constant even though changes occurred in the orientation or tilt of the chair.

Push-button microswitches used for subject control of the visual target motions were installed in the top of two hand grips attached to the gear ring structure on either side of the subject. Though not shown in Figures 1 and 2, a large lightproof housing fully enclosing the variable attitude chair was attached to the floor of the cradle to ensure that the visual target judgments were performed in complete darkness.

### Method

In the first half of this experiment each subject was oriented radially and given the task of estimating horizon by raising or lowering the linear displacement target. Each of the four subjects was then exposed to a run of the centrifuge at each of the five chair tilts:  $0^\circ$ ,  $15^\circ$  inboard,  $30^\circ$  inboard,  $15^\circ$  outboard, and  $30^\circ$  outboard for a total of five runs. The order in which the subjects were exposed to the various chair tilt angles, i.e., the morphological directions of the stimuli, was counterbalanced over the subjects. The acceleration magnitude profile of each run involved five different levels: 1.00, 1.25, 1.50, 1.75, and 2.00  $g$ . All subjects were first exposed to the static 1.00  $g$  stimulus to establish a baseline; two subjects then experienced the remaining accelerations in ascending order, the other two in descending order.

The actual experimental procedure was typically as follows: Initially, the centrifuge was at rest and the subject was seated in the variable attitude chair which was offset to one of the five stimulus direction angles. The subject then made his initial judgment of horizon, performed in complete darkness, by raising or lowering the luminous target. This data point was then recorded by the experimenter who thereupon instructed the subject to close his eyes. The visual target was then raised or lowered by the experimenter to a new position, the amount and direction of which was randomly programmed. The subject was then instructed to make a second judgment; a total of five such judgments constituted a single trial. The centrifuge was then slowly accelerated in the counterclockwise direction to the constant velocity required to establish the desired acceleration magnitude; at least 180 seconds were required to reach the initial velocity level. After a minimum stabilization period of 60 seconds at this constant angular velocity, the subject made five more judgments of horizon following the identical procedure used for the static case. Following these judgments, the centrifuge

velocity was changed to the next level; at least 90 seconds were required for the velocity transition. The subject judgments were repeated as before after 60 seconds had passed. Each run therefore required 25 subjective judgments leading to a total of 125 data points for each subject over the five runs. In the second half of the experiment, each subject was oriented tangentially and given the task of estimating his perception of vertical by means of the angular displacement target which could be rotated in either a clockwise (CW) or counterclockwise (CCW) direction. With this exception, the procedure was identical to that described for the first half of the experiment.

## RESULTS AND DISCUSSION

The basic elements of the mathematical notation used in this experiment and Experiment II to describe both the stimuli and responses are reviewed in each section of the results. Initially it should be noted, however, that the notation predicates that all of the acceleration stimuli be man-referenced to the  $x$ ,  $y$ , and  $z$  cardinal head axes in the direction sense as illustrated in Figure 3, in pictorial as well as in equation form. The  $x$ ,  $y$ , and  $z$  head axes denote the front-back, left-right, and vertex-base dimensions, respectively, of the skull while the frontal, sagittal, and horizontal head planes are mathematically identified as the  $yz$ ,  $xz$ , and  $xy$  planes of the head, respectively.

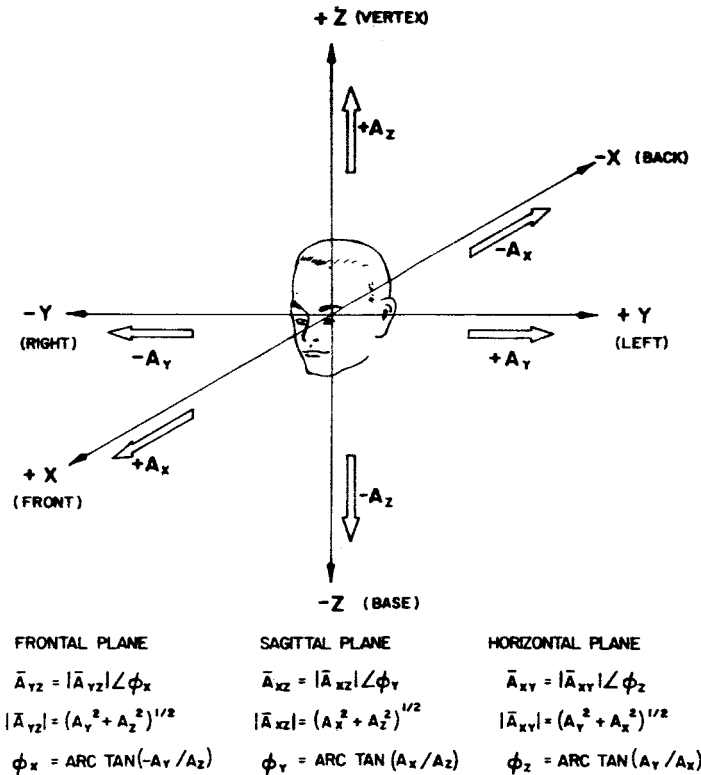


Figure 3

Basic notation and equations used to describe the cardinal  $x$ ,  $y$ , and  $z$  head axes and the related stimulus components where  $+A_x$ ,  $+A_y$ , and  $+A_z$  denote frontward, leftward, and upward directed accelerations of the head, respectively, in the kinematics sense of motion.

## Subjective Estimate of Horizon

The notation for the radial inboard orientation of the subject from which estimates of horizon were obtained is summarized in Figure 4 for one of the stimulus conditions. The schematic sketch at the left of this figure illustrates the cradle orientation during rotation where the variable attitude chair is at a fixed tilt 30 degrees outboard relative to the cradle axis C-C' which is perpendicular to the floor of the cradle. The cradle tilt angle, the angular deviation between C-C' and an Earth vertical axis V-V', is simply the angle whose tangent is equal to the ratio of the centripetal and gravitational accelerations. The resultant linear acceleration of the head in kinematics form is identified as a vector  $\bar{A}$  which always acts in the direction of the cradle axis C-C'.

### SUBJECT RADIAL

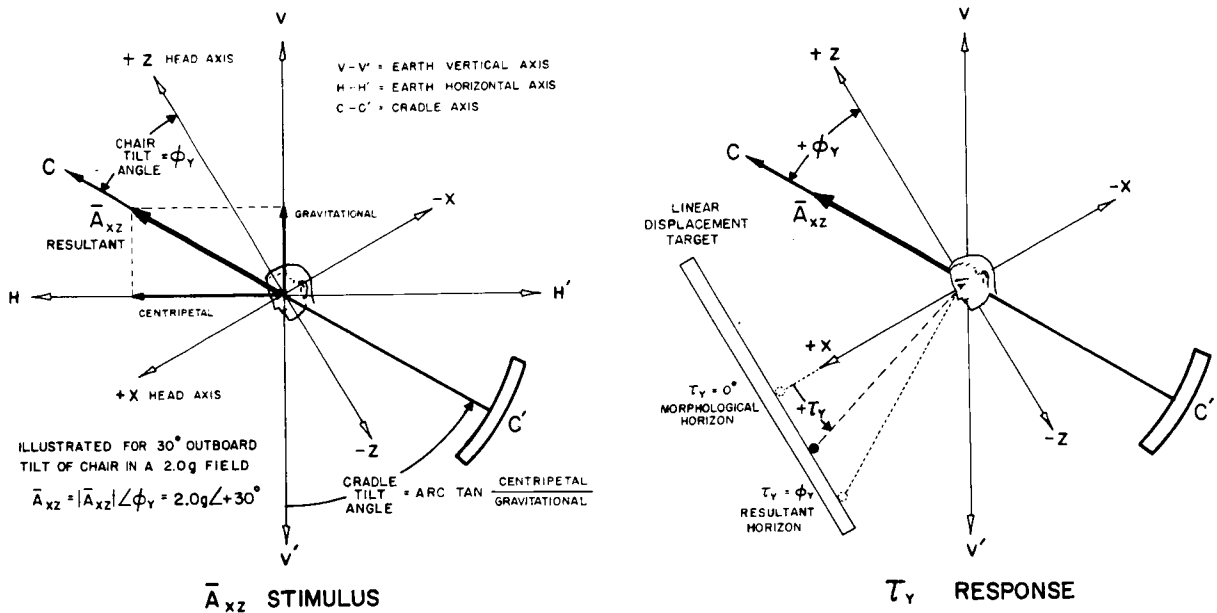


Figure 4

Basic stimulus and response elements of Experiment I for the radial orientation of the variable attitude chair with the subject facing inboard. The parameters of the variable magnitude, variable direction, static linear acceleration stimulus presented in the sagittal xz head plane are shown at the left: The  $\tau_Y$  angle used to quantify the elevation or depression of the Linear Displacement Target for the subjective perception of horizon judgment is identified at the right.

By using conventional vector shorthand notation, the magnitude and direction of  $\bar{A}$  can be separately identified as  $\bar{A} = |\bar{A}| \angle \phi$  where  $|\bar{A}|$  represents the absolute magnitude of  $\bar{A}$  and  $\phi$  the morphological direction of  $\bar{A}$  which, for this study, is simply the chair tilt angle.

To denote that this particular radial orientation of the subject results in changes of magnitude and direction of  $\bar{A}$  in the sagittal  $xz$  head plane, the stimulus is identified as  $\bar{A} = \bar{A}_{xz} = |\bar{A}_{xz}| \angle \phi_y$ . In effect, the  $xz$  subscript denotes that  $\bar{A}$  acts in the sagittal  $xz$  plane while the  $y$  subscript denotes that the directional changes in  $\bar{A}$  are equivalent to rotation of the  $\bar{A}_{xz}$  vector about the  $y$  (left-right) head axis. When the chair was tilted outboard,  $\phi_y$  was measured as a positive angle; when tilted inboard, as a negative angle. Thus  $\phi_y$  measures the angular deviation of the  $z$  head axis from the C-C' cradle axis along which  $\bar{A}_{xz}$  is always directed.

A similar side elevation view is shown at the right of Figure 4 to describe the procedure used to identify the motions of the linear displacement target. The vertical motions, as viewed by the subject, can be interpreted as being equivalent to rotation of the target about the  $y$  head axis. In a practical sense, the orientation of the target relative to the subject can be directly expressed in angular measurement units proportional to the angular deviation of the target above or below mean eye level even though the actual target motions are of pure translation form through application of simple trigonometric reduction. Specifically, the tangent of the target angle is the ratio of the measured linear displacement of the target proper above or below mean eye level to the measured distance between the eye and the target when positioned at mean eye level.

As illustrated in Figure 4, the symbol  $\tau_y$  (degrees) is used to denote the morphological orientation of the linear displacement target where  $\tau_y$  is measured as a positive angle when the target is below eye level and as a negative angle when above. When a subject places the target at the  $\tau_y = 0$  position, the target is at the objective morphological horizon; when the subject elevates or depresses the target to a  $\tau_y$  angle identical to the  $\phi_y$  direction angle, the target, and hence his subjective horizon, is at the resultant horizon defined by the resultant acceleration  $\bar{A}_{xz}$ .

It should be remembered that the target housing was rigidly fixed to the chair so that its orientation never changed relative to the subject even when the chair was tilted. Thus, identical  $\tau_y$  data points occurring with different chair tilt angles describe identical target positions or orientations relative to the subject.

To summarize, when the subject was seated radially, the stimulus was identified as  $\bar{A}_{xz} = |\bar{A}_{xz}| \angle \phi_y$  where  $|\bar{A}_{xz}|$  had five discrete values of 1.00, 1.25, 1.50, 1.75, and 2.00  $g$ ; and  $\phi_y$  had five discrete values equal to 0, +15, +30, -15, and -30 degrees where the plus and minus polarity signs denote the outboard and inboard tilts, respectively, of the chair.  $\tau_y$  measures the elevation or depression of the target above or below the horizontal plane of the head at eye level where  $\tau_y$  is positive when the subject moves the target below this plane and negative when he raises it above.



The subjective estimates of horizon data collected in the first part of the experiment where the subjects were seated facing radially inboard are listed in Table A1 of Appendix A for each of the four subjects as a function of the magnitude and direction parameters of the resultant linear acceleration stimuli presented in the sagittal  $xz$  plane of the head. Each  $\tau_y$  data listing represents the mean of five individual observations made at a given acceleration magnitude  $|\bar{A}_{xz}|$  and at a given morphological direction angle (chair tilt angle)  $\phi_y$ . The group means and pooled estimates of standard deviation representing twenty observations are also listed in Table A1.

The group means of the  $\tau_y$  measure of the subjective estimate of horizon are shown plotted in Figure 5 as a function of the absolute magnitude  $|\bar{A}_{xz}|$  of the acceleration stimulus for each of the five discrete  $\phi_y$  chair tilt angles. These data indicate that when the subject was sitting in a head erect posture relative to the stimulus,  $\phi_y = 0^\circ$ , an increase in acceleration magnitude resulted in an increased value of the  $\tau_y$  target angle used to objectively measure the subject's visual perception of horizon. In effect, each increase in acceleration level was accompanied by a further depression of the target below the horizon observed at the 1.00  $g$  level. When the subject was statically pitched back  $15^\circ$  and  $30^\circ$  toward the supine position ( $\phi_y = +15^\circ$  and  $\phi_y = +30^\circ$ ) relative to the stimulus, similar depressions of the subjective horizon data were noted. Importantly, the same observation holds when the subject was statically pitched  $15^\circ$

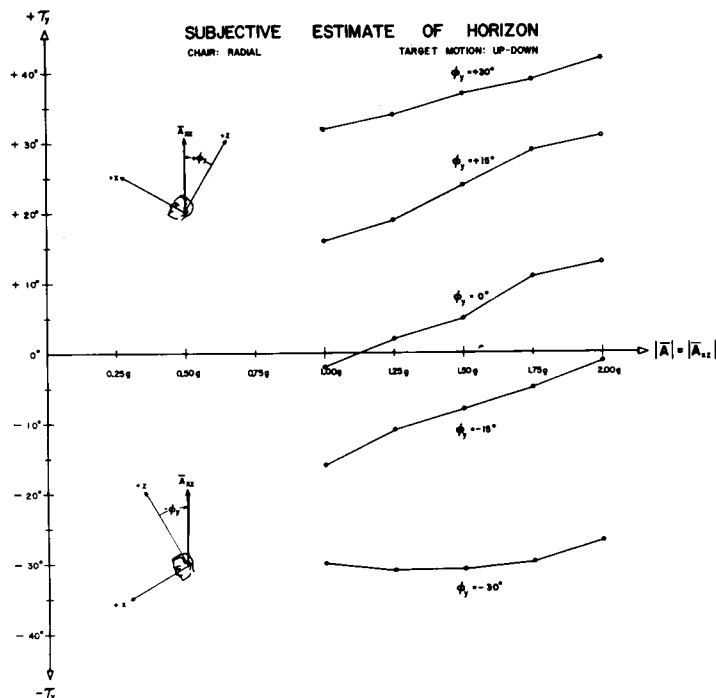


Figure 5

Mean estimates of subjective horizon ( $\tau_y$ ) as a function of resultant linear acceleration ( $|\bar{A}_{xz}|$ ) for various body tilts ( $\phi_y$ ). The effective direction of the resultant linear acceleration stimulus is shown schematically for positive and negative angles of body tilt. Stimulus magnitude does not influence subjective estimates of the horizon when body pitch angle,  $\phi_y$ , equals  $-30^\circ$ .

forward toward the prone posture ( $\phi_y = -15^\circ$ ). However, when the subject was pitched forward  $15^\circ$  further ( $\phi_y = -30^\circ$ ), his subjective estimate of horizon was much less affected by the increase in acceleration level.

These same  $\tau_y$  data are shown plotted in Figure 6 against the chair tilt angle  $\phi_y$  for the five different  $|\bar{A}_{xz}|$  acceleration magnitude levels. The dashed line denotes a perfect one-to-one correspondence of  $\tau_y$  and  $\phi_y$ . At this point it should be recognized that the chair tilt angle  $\phi_y$  is also an objective measure of the subject's horizon as delineated by the force element of the environment. Visualization of this horizon can be established by referring to the sketch at the right of Figure 4 where the subject is shown tilted backward  $30^\circ$ . The target will be at the resultant horizon in the force sense when it is lowered  $\phi_y$  degrees, i.e.,  $30^\circ$ , below eye level, so that it lies in a resultant horizontal plane (a plane perpendicular to the C-C' cradle axis along which  $\bar{A}_{xz}$  is directed) which intersects the head at eye level. Thus for any given chair tilt angle, the resultant horizon in the force sense is morphologically measured as  $\tau_y = \phi_y$  which never changes during a given run even though variations occur in the magnitude of the acceleration stimulus.

With this concept of the angle  $\phi_y$ , it can be appreciated from the data of Figure 6 that, except for the  $30^\circ$  pitch forward position ( $\phi_y = -30^\circ$ ), increases in acceleration

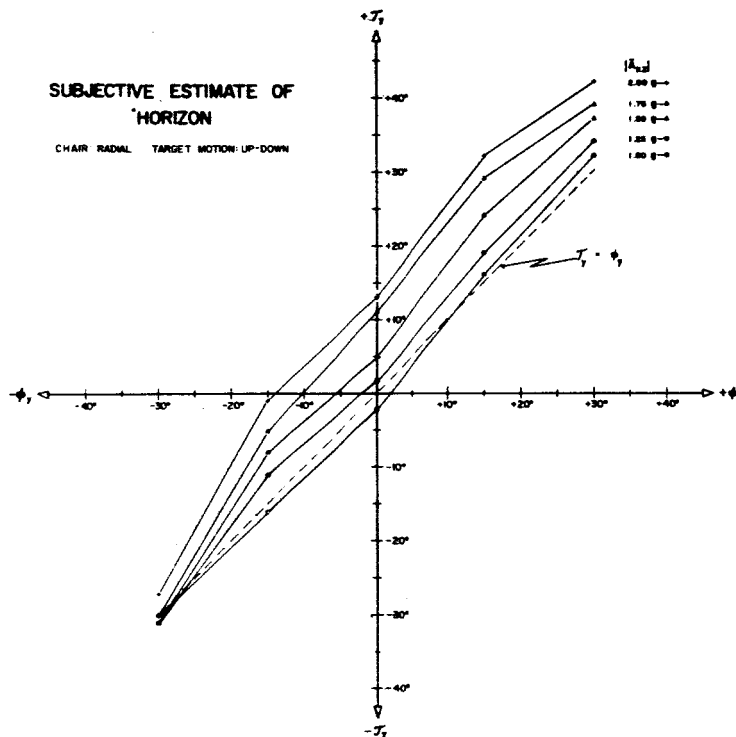


Figure 6

Mean estimates of subjective horizon ( $\tau_y$ ) as a function of actual tilt ( $\phi_y$ ) for various resultant linear accelerations ( $|\bar{A}_{xz}|$ ). The dashed line represents one-to-one correspondence of  $\tau_y$  and  $\phi_y$ . Note the convergence of the curves at  $\phi_y = -30^\circ$  for all magnitudes of resultant linear acceleration.

magnitude above the initial 1.00  $g$  level always resulted in subjective estimates of horizon ( $\tau_y$ ) which fell below the resultant horizon ( $\phi_y$ ) defined by the force environment. It is an obvious statement that subjective judgments at supra  $g$  levels were not keyed to true Earth horizon since the motion of the free-swinging cradle assembly and the variable attitude chair continually altered the spatial orientation of the subject relative to the Earth's surface. That is to say, the vertical and horizontal spatial dimensions defined by the Earth's gravitational action no longer described the directional characteristics of the environment in a force sense.

To facilitate statistical analysis, the basic data were coded by subtracting the objective resultant horizon measure, defined by  $\phi_y$ , from the subjective estimate of horizon  $\tau_y$  data to obtain an error score. Variance analyses were performed on the error data and the results are presented in Table B1 of Appendix B. From these calculations, it may be verified that an increase in acceleration magnitude significantly influences error in estimation of horizon ( $F = 38.52$ ,  $df = 4/60$ ,  $P < .001$ ). To investigate the linearity of the variations arising in  $\tau_y$  as acceleration magnitude was increased, a trend analysis for error was performed for each chair tilt value. These results, also presented in Table B1, indicate that error in estimates of horizon increase linearly with the increases in acceleration level for all chair tilt angles except  $\phi_y = -30^\circ$ .

For the conditions where the head was pitched forward  $15^\circ$  and  $30^\circ$  relative to the acceleration field, the data of this study are in essential agreement with those of Schöne (9). His data indicated that minimal changes occurred in the estimate of horizon when the subject was inclined approximately  $24^\circ$  forward. The present study showed the "null" or "insensitive" axis of response where the subjects could accurately estimate their horizon without perturbations due to changes in acceleration level to be in the vicinity of  $\phi_y = -30^\circ$ . However, for the pitch backward inclinations ( $\phi_y = +15^\circ$ ,  $\phi_y = +30^\circ$ ) which were outside the range of those Schöne investigated, the data indicated direct conflict with the linear equation he postulated to relate the subjective estimate of horizon to the force component acting in only a single direction of the receptor, i.e., "shear in the utricle."

Recognition of the conflict may be established in part by referring to the data of the present study as plotted in Figure 5. Schöne showed that when his response data measured over the 1.00  $g$  to 2.00  $g$  range were linearly projected to the zero acceleration level ( $\bar{A}_{xz} = 0$  in Figure 5), all lines intersected the  $\tau_y$  subjective estimate of horizon ordinate near the  $\tau_y = -24^\circ$  value. If the data of Figure 5 were projected to the ordinate, essential agreement would obtain for  $0^\circ$  tilt and for forward pitches of  $15^\circ$  and  $30^\circ$ . However, the linear projection of the backward pitch data ( $\phi_y = +15^\circ$ ,  $\phi_y = +30^\circ$ ) would be in pronounced disagreement. In effect, for this study when the shear force was held constant at some value other than zero, and the compression force varied, changes in the subjective estimates of horizon were noted. Later in this discussion, a new mathematical analog of otolith function will be formulated to eliminate the conflicts between the data of these two studies.

A point of experimental interest arises from the data of Figure 5 when one compares the directional nature of  $\tau_y$  for the  $15^\circ$  pitch backward ( $\phi_y = +15^\circ$ ) and the  $15^\circ$  pitch forward ( $\phi_y = -15^\circ$ ) orientations of the subject. For each direction of inclination the subject always lowered the target as acceleration magnitude increased; this is equivalent to stating that his subjective estimate of horizon was lowered as the strength of his force field increased. When such subjective estimates are made using the visual process, it is questionable as to what effect simultaneous stimulation of the tactile receptors of the body may have on the subject's judgments. From the pure empirical viewpoint it might be said that if a subject is tilted backward, and the strength of the force field increased, he will feel, knowingly or unknowingly, as if he were tilted further back and therefore lower his estimate of horizon as a result of the postural or tactile elements. Similarly, if he were pitched forward and the force field increased, he would feel that he was tilted even further forward and thus raise his estimate of horizon.

Not arguing the strength, or even the validity, of such a viewpoint, it can be noted from the  $\phi_y = +15^\circ$  and  $\phi_y = -15^\circ$  data of Figure 5 that the subjective visual estimate of horizon was lowered for the pitch forward orientation as well as for the pitch backward posture. If it were assumed that the tactile influence is significant, then one would also be forced to conclude that the tactile receptors as a whole also have a null or insensitive axis which is inclined approximately  $30^\circ$  forward from the longitudinal axis of the head-torso. This particular radial orientation of the subject offers, therefore, an interesting experimental approach to differentiating between labyrinthine normal and abnormal subjects where the latter are assumed to have primarily tactile response, e.g., by exposing both types of subjects to successive  $15^\circ$ ,  $30^\circ$ , and  $45^\circ$  pitch forward inclinations and measuring their subjective estimates of horizon for different levels of acceleration. If Schöne's data are accepted, forward inclinations beyond the  $30^\circ$  null axis of response would result in an elevation of subjective horizon as acceleration is increased. If the responses for a normal subject were then plotted as in Figure 5, the  $-15^\circ$ ,  $-30^\circ$ , and  $-45^\circ$  positions would result in curves of positive, zero, and negative slope, respectively. Since one could not safely assume that the response curves of a labyrinth-defective subject relying on tactile cues would follow the same progression, the potential for the development of a definitive otolith function test is real.

### Subjective Estimate of Vertical

The notation used to describe the stimulus-response parameters of this portion of the experiment, summarized in Figure 7, is identical to that of the first half except for the subscripts. Since  $\bar{A}$ , for the tangential orientation, changes direction and magnitude in the frontal ( $yz$ ) head plane, the stimulus is identified as  $\bar{A} = \bar{A}_{yz} = |\bar{A}_{yz}| \angle \phi_x$  where the  $x$  subscript denotes the equivalent rotation of  $\bar{A}$  about the  $x$  head axis. As before, five stimuli conditions were chosen for the magnitude of the stimulus, i.e.,  $|\bar{A}_{yz}| = 1.00, 1.25, 1.50, 1.75$ , and  $2.00 g$ , and five conditions for the direction, i.e.,  $\phi_x = 0, +15, +30, -15$ , and  $-30$  degrees where  $\phi_x$  was measured as a positive angle when the chair tilt was outboard, and negative when inboard.

## SUBJECT TANGENTIAL

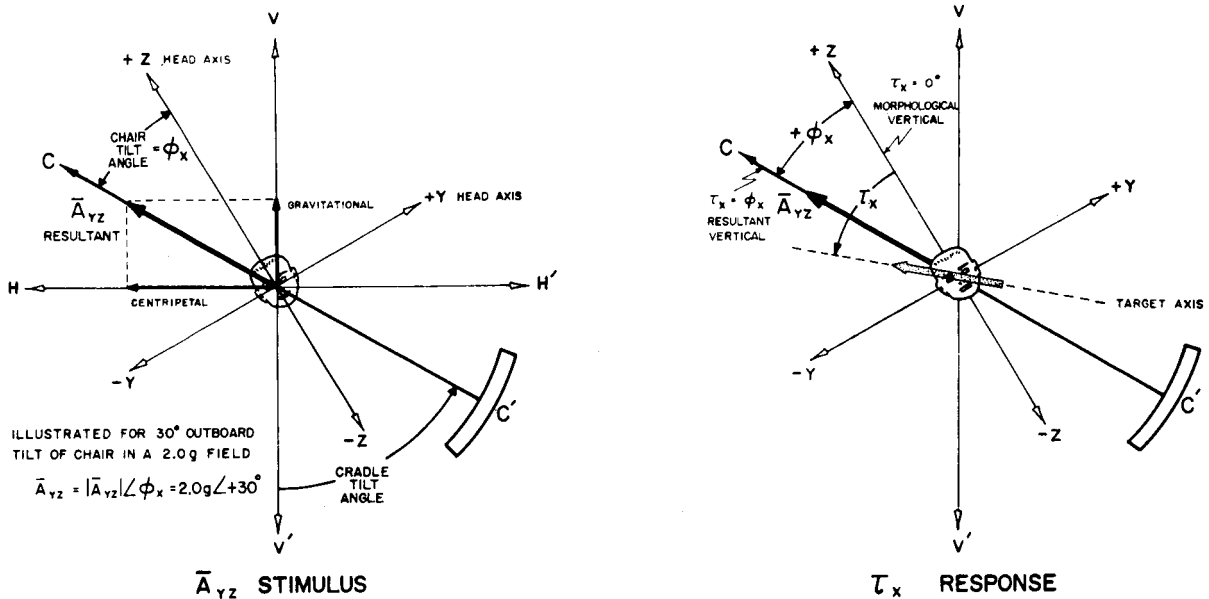


Figure 7

Basic stimulus and response elements of Experiment I for the tangential orientation of the variable attitude chair with the back of the subject in the direction of centrifuge rotation. The parameters of the variable magnitude, variable direction, static linear acceleration stimulus presented in the frontal  $yz$  head plane are shown at the left: The  $\tau_x$  angle used to quantify the CW or CCW angular displacement of the Digital Angular Position Target for the subjective perception of vertical is identified at the right.

The subjective estimate of vertical data collected in the second part of this experiment where the subjects were seated tangentially with their backs in the direction of the counterclockwise rotation of the centrifuge are listed in Table A2 of Appendix A for each of the four subjects as a function of the magnitude and direction of the acceleration stimulus presented in the frontal  $yz$  head plane. As with the first part of the experiment, each  $\tau_x$  data listing in this table represents the mean of five individual observations made at a given acceleration magnitude  $|\bar{A}_{yz}|$  and a given  $\phi_x$  chair tilt angle. The group means and pooled standard deviations for all subjects combined are also listed in the table.

The group means of the  $\tau_x$  measure of the subjective estimate of vertical are shown plotted as a function of the acceleration magnitude for each of the five  $\phi_x$  chair

- tilt angles in Figure 8. Positive values of  $\phi_x$  indicate that the subject was tilted toward his left relative to the direction of the force field while negative values indicate a tilt to the right. As noted in Figure 7, the target is objectively aligned with morphological vertical ( $z$  axis of the head) when  $\tau_x = 0^\circ$  and objectively aligned with the resultant vertical defined by  $\bar{A}_{yz}$  when  $\tau_x = \phi_x$ . Positive values of the  $\tau_x$  response denote that the subject oriented the visual line target so that it was rotated clockwise relative to the longitudinal axis ( $z$  head axis) of the body as viewed by the subject; negative  $\tau_x$  angles describe a counterclockwise displacement of the target. These data indicated that when the subject was seated in a head erect posture relative to the force field ( $\phi_x = 0^\circ$ ), his judgments of vertical were relatively unaffected by changes in acceleration magnitude. When the subject was tilted to his left ( $\phi_x = +15^\circ$  and  $\phi_x = +30^\circ$ ) and exposed to accelerations of increasing level, increased values of  $\tau_x$  in the positive or clockwise direction were observed. Similarly, when the subject was tilted toward his right ( $\phi_x = -15^\circ$  and  $\phi_x = -30^\circ$ ) and acceleration level increased, increased values of  $\tau_x$  in the negative or counterclockwise direction were observed. In general, except for the head erect posture, an increase in acceleration magnitude resulted in the subject moving the target further away from his longitudinal head axis whether he was tilted left or right.

These  $\tau_x$  judgment data are also shown plotted against the  $\phi_x$  chair tilt angle for the five different  $|\bar{A}_{yz}|$  acceleration magnitudes in Figure 9. If it is recalled that the chair tilt angle  $\phi_x$  also denotes the orientation of resultant vertical, it becomes apparent that the data of Figures 8 and 9 show that, except for the head erect posture, the subject group consistently moved the target beyond true resultant vertical when the magnitude of the acceleration stimulus was increased. These results can also be described in terms of the Aubert (A-) and Müller (E-) phenomena (8). An A-phenomenon is experienced when a subject, tilted about his  $x$  head axis, perceives a visual target which is in fact aligned with resultant vertical as being inclined in the direction away from his body tilt. If the subject were given control of the target motions, he would rotate the target toward his body to establish his visual estimate of vertical. With the  $\tau_x$  and  $\phi_x$  notations of this study, the A-phenomenon is observed when the  $\tau_x$  judgment angle is less than the  $\phi_x$  angle which denotes resultant vertical. In other words, the subject's  $\tau_x$  placement of the target is an underestimation of the actual location of resultant vertical. Similarly, the E-phenomenon is experienced when a subject, tilted about his  $x$  axis, perceives a visual target again aligned with resultant vertical as being inclined in the direction toward his body. The subject then would rotate the target away from his body so that  $\tau_x$  is greater than  $\phi_x$ , representing a placement of the target which overestimates the actual location of resultant vertical relative to the head.

From this viewpoint, it can be said from the data of Figures 8 and 9 that at the normal 1.00  $g$  level, the subject group was quite capable of estimating resultant vertical with minimal error, and that the small deviations that did occur were generally in the direction of the A-phenomenon since  $\tau_x$  was less than  $\phi_x$  for all chair tilt angles except  $\phi_x = +15^\circ$  where  $\tau_x = +15.5^\circ$ . However, except for the head erect posture, when the acceleration level was increased, the subjective estimates of vertical consistently

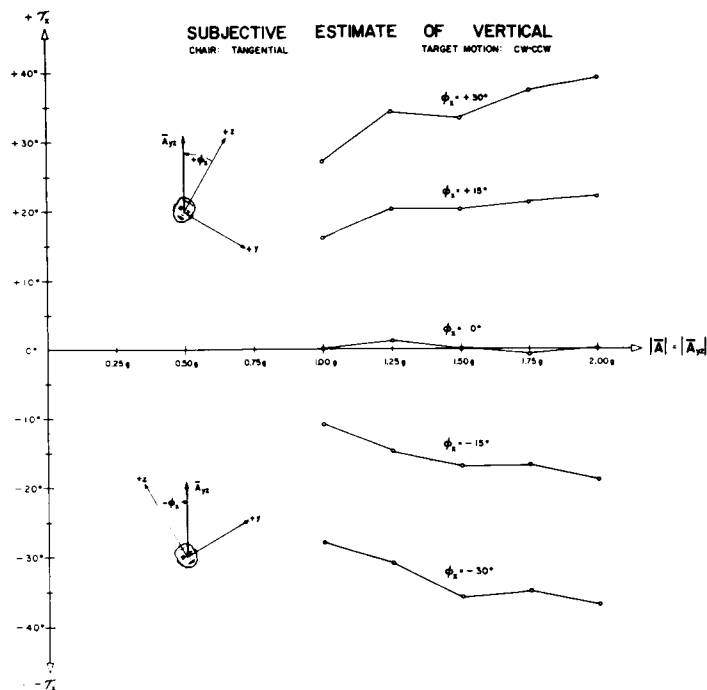


Figure 8

Mean estimates of subjective vertical ( $\tau_x$ ) as a function of resultant linear acceleration ( $|\bar{A}_{yz}|$ ) for various body tilts ( $\phi_x$ ). The effective direction of the resultant linear acceleration stimulus is shown schematically for positive and negative angles of body tilt. Subjective estimates of the vertical are independent of stimulus magnitude when the body roll angle,  $\phi_x$ , equals zero degrees.

increased in the direction of the E-phenomenon. This is observed in Figure 9 where it may be seen that the bulk of the  $\tau_x$  data lies above the dashed  $\tau_x = \phi_x$  locus for positive  $\phi_x$  chair tilt angles and below the locus for negative chair tilt angles when acceleration is increased. In essence, the absolute magnitude of the subjective estimate of vertical  $|\tau_x|$  becomes greater than the absolute magnitude of the true resultant vertical  $|\phi_x|$ .

As with the  $\tau_y$  horizon data, variance analyses were performed on error scores obtained by subtracting the  $\phi_x$  measure of resultant vertical from the  $\tau_x$  subjective judgments. The results, listed in Table B2, statistically confirm the point that the magnitude of the acceleration stimulus acting in the sagittal plane significantly affected the subjective estimate of vertical ( $F = 25.15$ ,  $df = 4/60$ ,  $P < .001$ ). Also listed in this table are the results of a trend analysis of error in estimation of vertical as a function of increase in magnitude for each of the five tilt angles. The error in estimation of vertical increased linearly, though not so markedly as that observed with the horizon data, for all tilt angles except  $\phi_x = 0$ . This exception is in agreement with the findings of Colenbrander (1) who found an absence of eye counterroll for the head erect posture when the acceleration acting in the frontal plane of the head along the  $z$  axis was raised from 1.00 to 2.00  $g$ , and with those of Schöne (9) and Miller and Graybiel (7) for subjective judgments of the vertical and horizontal under similar conditions. Just as the horizon data indicated a null axis of  $\phi_y = -30^\circ$  in the sagittal plane of the head where an

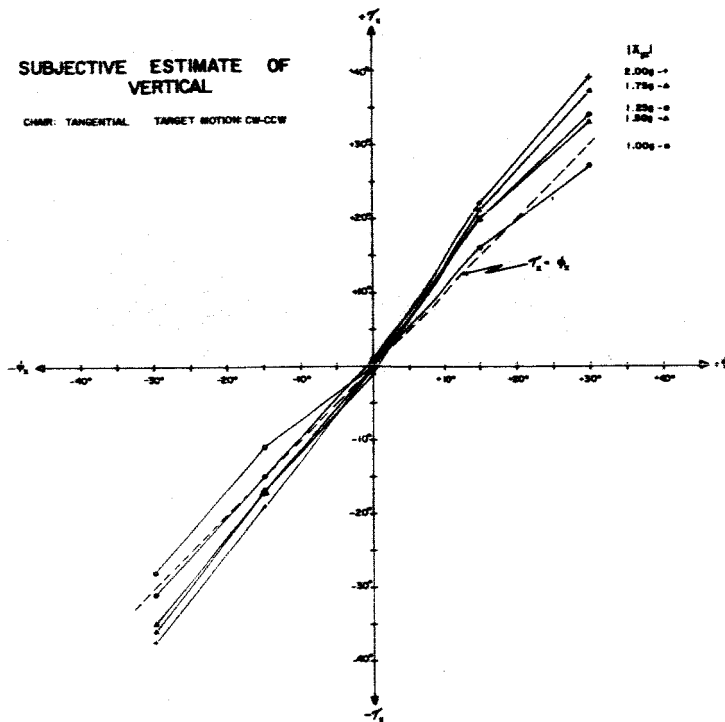


Figure 9

Mean estimates of subjective vertical ( $\tau_z$ ) as a function of actual tilt ( $\phi_z$ ) for various resultant linear accelerations ( $|\bar{A}_{yz}|$ ). The dashed line represents perfect estimation.

increased force environment did not influence perception of horizon or attitude in space, these vertical data suggest an identical relationship in the frontal plane except that the null axis is directed along the longitudinal axis ( $\phi_x = 0^\circ$ ) of the head.

## EXPERIMENT II

### PROCEDURE

#### Subjects

Four men, two of whom (MJC and JIN) had served as subjects in Experiment I, were used in the present experiment. Prior to the test runs all subjects had received several familiarization runs with the experimental apparatus.

#### Apparatus

As with Experiment I, the previously described centrifuge, free-swinging cradle, and variable attitude subject-chair served as the basic apparatus. Essentially, the only difference involved replacement of the helmet-type head holder with a two-piece



Fiberglas shell, which was custom-molded to the head-torso contours of each individual subject, to provide improved constraint to the variable attitude chair. Front and side views of typical shells are shown in Figure 10. Permanent installation of two, force-balance type linear accelerometers on the side of the head plate used to hold the head-torso shell to the variable attitude chair permitted real time measurement of the magnitude and direction of the resultant linear acceleration stimulus presented to each subject. When the subject was seated radially, the accelerometer signals measured the linear accelerations acting along the  $x$  and  $z$  head axes as depicted in the photograph of Figure 11; when seated tangentially, the accelerometers were rotated to measure the accelerations along his  $y$  and  $z$  head axes.

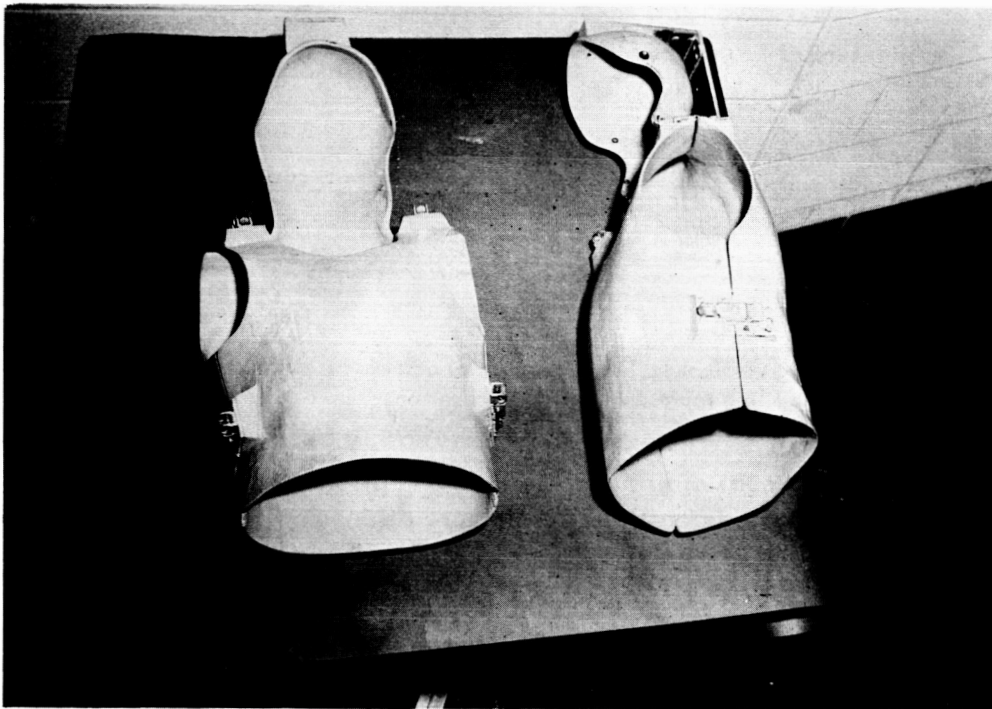


Figure 10

Front and side views of integral Fiberglas body molds used for protection and restraint of subject.

Lastly, a new target assembly, the details of which are discussed in Appendix C, permitted target motion with two degrees of freedom. The visual element of the target was in the form of a luminous cross with horizontal and vertical crossarms 1 inch long and 1/32nd inch wide. The target housing was attached to the instrument rack so that it was directly in front of the subject at eye level. The plane in which the motions of the cross target occurred was parallel to the frontal  $yz$  head plane of the subject. The vertical and horizontal positions of the target were derived from digital voltmeter readouts of position command signals derived from independent subject and experimenter controlled potentiometers. Bias controls at the central console allowed the experimenter to program random vertical and horizontal target displacement offsets following each subject judgment.

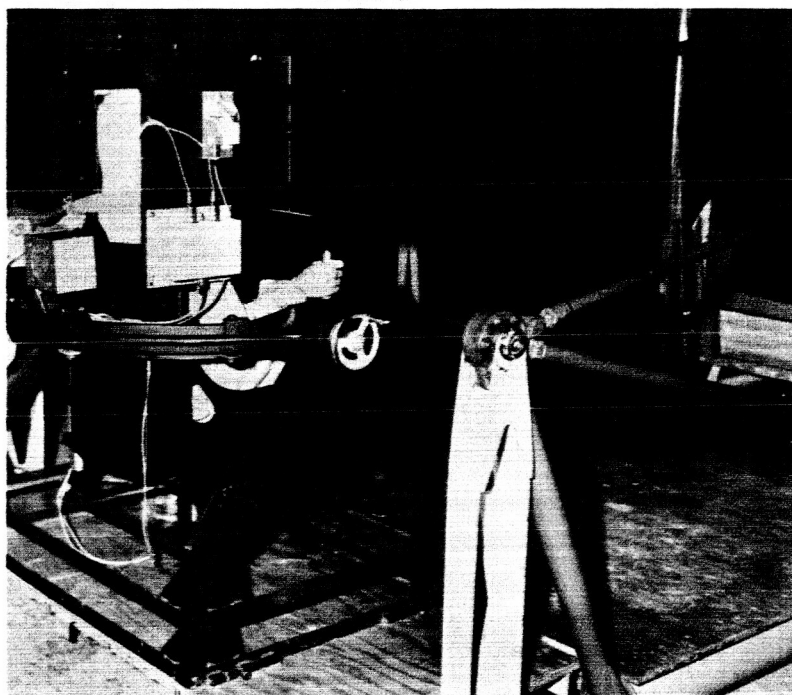


Figure 11

View showing position of orthogonally mounted linear accelerometers used to measure linear accelerations acting along subject's  $x$  and  $z$  head axes.

### Method

This experiment, which dealt with egocentrically referenced judgments of visual target orientation, was carried out in three distinct phases. The first two phases involved the use of the two-dimensional target where the response task was to place the target cross in a visually dead ahead position, that is, at the projected intersection of the mid-sagittal head plane and the horizontal head plane at eye level. In the first phase the subject was oriented radially; in the second, tangentially. In both cases the acceleration magnitudes and directions were the same as those denoted in Experiment I except that the  $2.00 g$  level was omitted. Prior to each test run, zero baselines for the two-dimensional target were established by moving the target cross to eye height as measured with a level and then having the subject move the target cross left or right so as to be subjectively centered. The electrical system was then adjusted so that zero deviation about the horizontal and vertical dimensions was recorded by the digital voltmeter. The test run procedure described for Experiment I was then followed.

For the third phase of the experiment, four acceleration levels but only three chair offset angles were used. With tangential orientation the stimulus acceleration acted in the frontal  $yz$  head plane and consisted of  $1.00$ ,  $1.25$ ,  $1.50$ , and  $1.75 g$  acceleration levels at  $0^\circ$ ,  $+30^\circ$ , and  $-30^\circ$  chair tilt angles. Each subject was required to align the long dimension of the previously described angular position target to his longitudinal body axis as defined by the  $z$  head axis.

## RESULTS AND DISCUSSION

### Subjective Estimate of Visual Dead Ahead

Subjective estimates of the visual dead ahead orientation of the luminous cross for each subject and the combined group means for all subjects are presented in Tables A3-A6. The target was placed at the objective dead ahead position,  $\tau_y = 0$ ,  $\tau_z = 0$  when the center of the luminous cross fell at the projected intersection of the mid-sagittal head plane and a horizontal head plane at eye level. As in Experiment I, positive values of the  $\tau_y$  target angle indicate that the subject placed the target below this horizontal plane; negative values indicate that it was placed above the plane. Positive values of  $\tau_z$  indicate that the subject placed the target to the left of the visual dead ahead plane; negative values indicate that the target was positioned to the right.

The  $\tau_y$  and  $\tau_z$  group mean data listed in Tables A3 and A4 for the subject facing radially inboard are shown plotted in Figures 12 and 13 as a function of the absolute magnitude of the  $\bar{A}_{xz}$  linear acceleration stimulus acting in the sagittal  $xz$  head plane for each of the five  $\phi_y$  chair tilt angles. From these figures it may be seen that whether the subjects were pitched forward or backward relative to the stimulus, their

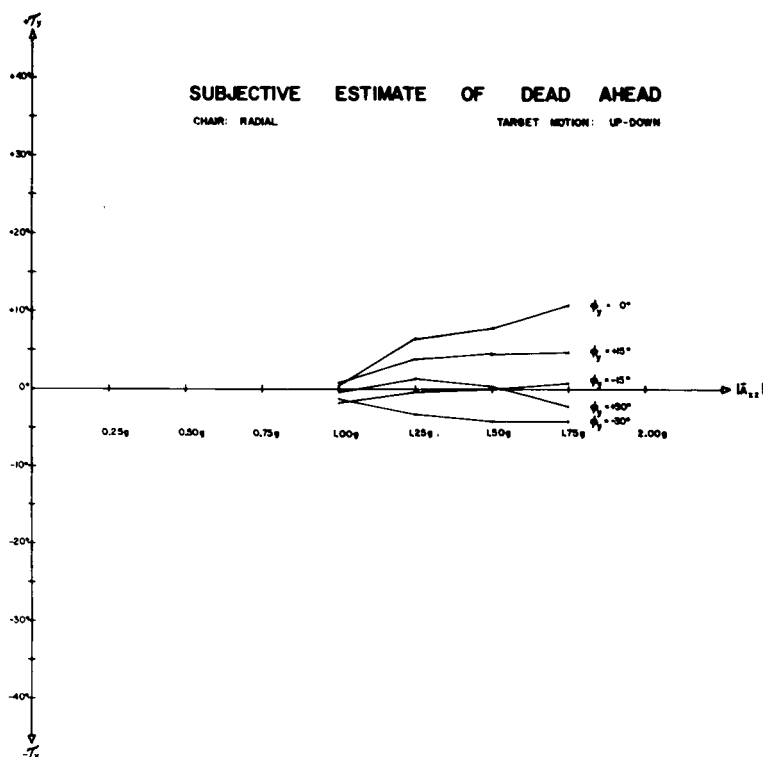


Figure 12

Mean estimates of subjective dead ahead as a function of resultant linear acceleration ( $|\bar{A}_{xz}|$ ) for various body tilts ( $\phi_y$ ). The data represent vertical adjustments ( $\tau_y$ ) of the target cross.

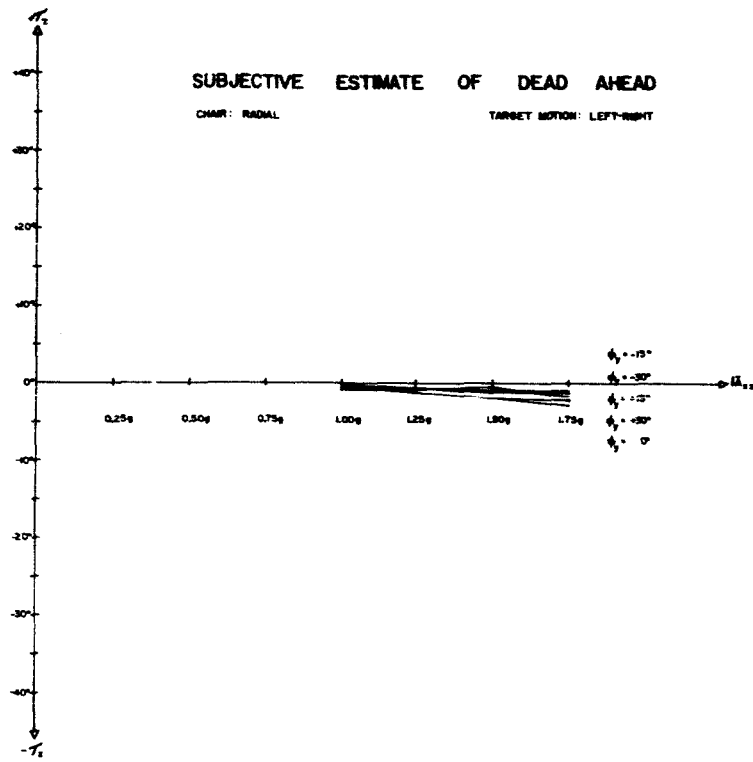


Figure 13

Mean estimates of subjective dead ahead as a function of resultant linear acceleration ( $|\bar{A}_{xz}|$ ) for various body tilts ( $\phi_y$ ). The data represent horizontal adjustments ( $\tau_z$ ) of the target cross.

judgments were relatively unaffected by changes in magnitude of the acceleration; in addition, their  $\tau_y$  and  $\tau_z$  judgments closely approached the objective dead ahead position referenced to the 1.00 g level. This also applies for the  $\tau_z$  judgments in the horizontal dimension for the  $\phi_y = 0$  head erect orientation. Such was not the case for the vertical adjustments of the target  $\phi_y = 0$  since increases in acceleration magnitude resulted in a depression of the target below the dead ahead level.

Summaries of variance analyses of these data are presented in Tables B3 and B4. It would seem from the significant over-all F ratio that acceleration magnitude influences the amount of deviation in the  $\tau_y$  estimation of dead ahead in the vertical dimension ( $F = 6.82$ ,  $df = 3/45$ ,  $P < .001$ ). However, when additional analyses were performed for each  $\phi_y$  chair tilt angle, it was observed that only at the zero tilt orientation ( $\phi_y = 0$ ) was a significant main effect in  $\tau_y$  target adjustment ( $F = 36.14$ ,  $df = 3/9$ ,  $P < .001$ ) produced by a change in acceleration magnitude. For errors in the horizontal dimension, no difference was observed between acceleration magnitude and  $\tau_z$  deviations from dead ahead.

The  $\tau_y$  and  $\tau_z$  group mean data listed in Tables A5 and A6 for the subject seated tangentially with his back in the direction of rotation are shown plotted in Figures 14 and 15 as a function of the absolute magnitude of the  $\bar{A}_{yz}$  linear acceleration stimulus acting in the frontal  $yz$  head plane for each of the five  $\phi_x$  chair tilt angles. From

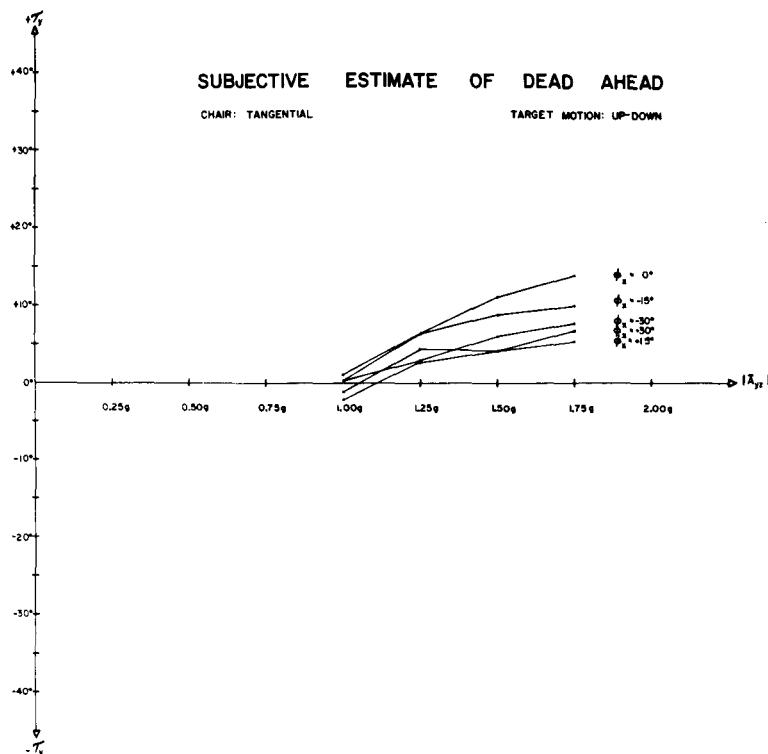


Figure 14

Mean estimates of subjective dead ahead as a function of resultant linear acceleration ( $|\bar{A}_{yz}|$ ) for various body tilts ( $\phi_x$ ). The data represent vertical adjustments ( $\tau_y$ ) of the target cross.

Figure 14, it may be seen that changes in acceleration level were accompanied by changes in the  $\tau_y$  measure of subjective dead ahead in the vertical dimension. These changes occurred whether the subject was tilted toward his left ( $+\phi_x$ ), tilted toward his right ( $-\phi_x$ ), or maintained erect ( $\phi_x = 0$ ) relative to the acceleration stimulus. From the plot of the  $\tau_z$  data shown in Figure 15, it can be seen that, as with stimulation in the sagittal  $xz$  head plane, changes in acceleration magnitude had little effect on subjective estimation of the horizontal dimension of visual dead ahead. Summary variance analyses of these  $\tau_y$  and  $\tau_z$  data are presented in Tables B5 and B6 where it is statistically established that changes in acceleration magnitude did significantly influence the  $\tau_y$  vertical dimension of dead ahead ( $F = 10.29$ ,  $df = 3/45$ ,  $P < .001$ ) but had little effect on the estimate of the horizontal dimension ( $F = 2.74$ ,  $df = 3/45$ ,  $P > .05$ ). When separate analyses were performed, significant linear relationships were found between the changes in the  $\tau_y$  measure of target depression and the changes in acceleration magnitude, the deviation below the objective dead ahead plane always increasing with increasing magnitude.

The results of these first two phases of Experiment II, both of which involved identical subjective judgment tasks egocentrically keyed to the visual dead ahead morphological reference, can be summarized as follows: The group was consistently capable of placing the luminous cross quite closely to the visual dead ahead position

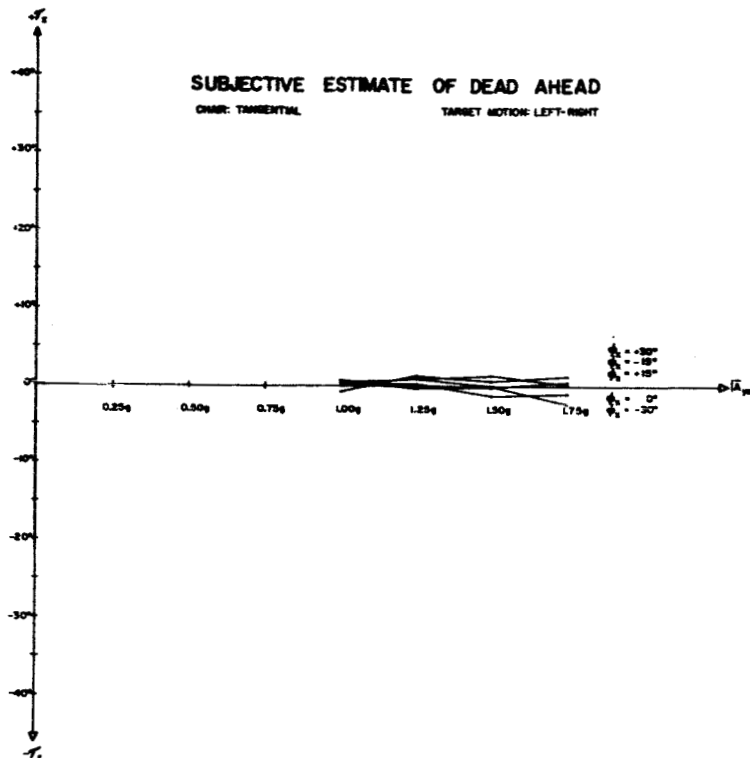


Figure 15

Mean estimates of subjective dead ahead as a function of resultant linear acceleration ( $|\bar{A}_{yz}|$ ) for various body tilts ( $\phi_x$ ). The data represent horizontal adjustments ( $\tau_x$ ) of the target cross.

in the  $\tau_z$  horizontal dimension where the target was located essentially at the center of the eyes; these judgments were not affected by either changes in the magnitude of the acceleration stimulus, changes in the direction (chair tilt angle) of the stimulus within a given head plane, or by the head plane, sagittal or frontal, in which the stimulus variations occurred. These parameters did, however, affect the  $\tau_y$  estimates of the vertical dimension of dead ahead for the group. When the subjects were oriented radially, the target was depressed below the objective dead ahead position as acceleration was increased with zero chair tilt ( $\phi_y = 0$ ). When the subjects were pitched backward or forward from this head erect posture, their judgments were no longer affected by changes in acceleration level. When the subjects were oriented tangentially so that stimulation occurred in the frontal head plane, increases in acceleration magnitude resulted in a depression of the target for the head erect orientation as well as the tilt-left or tilt-right attitudes.

### Subjective Estimate of Morphological Vertical

As in the case of estimation of vertical in Experiment I defined by the  $z$  head axis, the angular position of the target was denoted as  $\tau_x$  degrees where positive or negative angles result if the target is rotated clockwise or counterclockwise, respectively, from its original  $\tau_x = 0$  alignment with the  $z$  head axis as viewed by the subject.

Subject response data and related statistics derived from the third phase of the experiment are listed in Tables A7 and B7 where the judgment task involved the alignment of the angular position target with the morphological vertical ( $z$  head axis) while the subject was seated tangentially with the back in the direction of rotation. The  $\tau_x$  group mean data are shown plotted in Figure 16 as a function of acceleration magnitude  $|\bar{A}_{yz}|$  in the frontal head plane for three different chair tilt orientations. As in Experiment 1,  $\tau_x = 0$  when the long dimension of the target is aligned with the longitudinal  $z$  head axis.  $\tau_x$  was measured as a positive angle when the target rotated CW from this alignment as viewed by the subject; as a negative angle when rotated CCW.

From the data of Figure 16 and the related statistical analysis calculations of Table B7, it can be seen that the group was quite capable of estimating the morphological body axis without being influenced by either the magnitude or direction of the frontal plane acceleration stimulus. Supporting these data were reports from each subject when using the two-dimensional target that no apparent tilts of the luminous cross target were observed at any acceleration level or chair tilt when in the tangential alignment.

The observed differences in trend of the absolute (subjective vertical judgments of Figure 8) and the egocentric ( $z$  body axis judgments of Figure 16) localization estimates

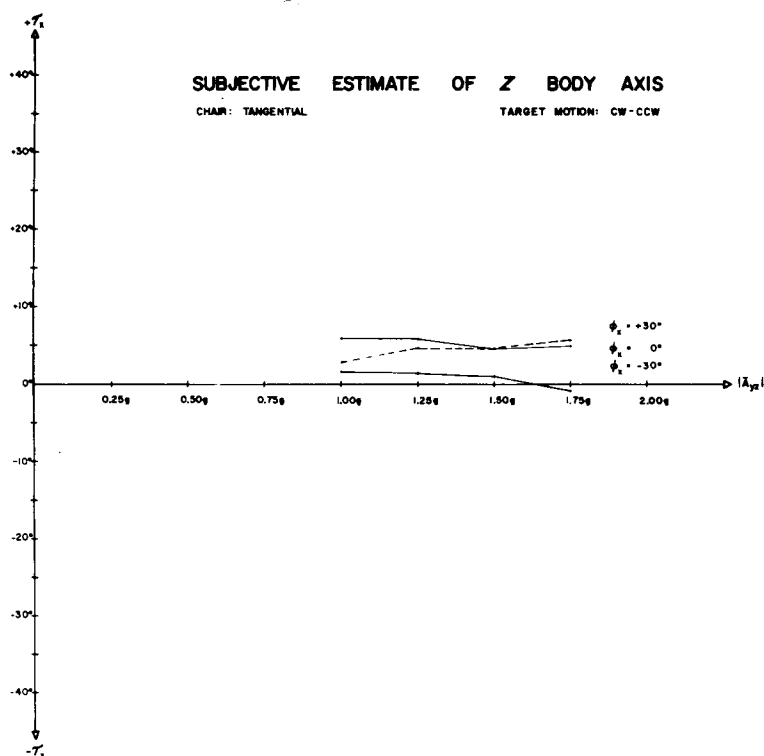


Figure 16

Mean estimates of subjective  $z$  body axis as a function of resultant linear acceleration ( $|\bar{A}_{yz}|$ ) for various body tilts ( $\phi_x$ ). The data represent rotary alignments ( $\tau_x$ ) of the Angular Position Target by the subject to his longitudinal axis. Note that at all body tilts judgments are independent of stimulus magnitude.

as a function of stimulus magnitude at various body tilts are of some interest in connection with speculations on the part ocular counterrolling may play. It has been considered that errors in both these judgments during lateral inclinations may arise in part from counterrolling (10, p 209). Since ocular counterrolling has been shown to increase as a function of stimulus magnitude and if it enters into both judgments, one would expect both the subjective vertical and the  $z$ -body axis judgment to vary. However, it should be noted that the intensity of the force field had minimal effect on the visual perception of the morphological  $z$  axis.

These data have further implications of considerable interest for the design of experiments to be performed in weightless flight or in space laboratories with weightlessness or subgravity as an operational characteristic. Assume, for example, that an upright subject is required, during subgravity, to adjust a target either to the environmental vertical defined by the existing resultant force or to the morphological vertical defined by his body  $z$ -axis. From Figures 8 and 16 it is apparent that the data predict there will be no significant deviation of either criterion at a zero degree offset. Neither, if the criterion selected is the morphological vertical, will offsetting the subject by right or left tilt up to at least  $30^\circ$  result in target deviations. When, however, a force reference is chosen, target deviation will vary as a function of body tilt with respect to it.

If an individual is exposed to zero or very near zero gravity rather than subgravity environments, extrapolation of the curves of Figures 8 and 16 would lead to a prediction of no target shift for either criterion. Insofar as the subjective estimate of vertical is concerned, in the static weightless environment, force is nonexistent, and in this sense, the word tilt has no meaning whatsoever, whether we speak of the biological mechanism as a whole or of its individual receptors. Since the extracorporeal reference is nonexistent, the judgment of vertical in a force sense is indeterminate. At most, a subject could be instructed, or if not so instructed would naturally tend to align such a target with a nonforce element of his environment, typically the axes of his vehicle. With this type of task and with man and vehicle in fixed orientation relative to each other, the judgment would in essence be the determination of the morphological vertical or horizontal.

This interpretation is supported by the experiments of Hammer (2) who placed a subject upright and facing backward and then obtained judgments of the subjective vertical during exposure to parabolic aircraft trajectories. As would be predicted from the present data, target deviation was essentially zero, ranging from  $0.68^\circ$  at  $1.00g$  to  $1.49^\circ$  at  $0g$ . The subject's orientation in the aircraft was such that throughout the subgravity portion of the parabola, he was in alignment with the resultant force, i.e., at zero body tilt. From Figure 8 one would not expect any marked target deviation. In the zero gravity portion, there was again no target deviation observed, a result predictable from the data of Figures 8 and 16. It is of interest to note that Hammer also concludes: "... tactile contact with seat and head rest and various kinesthetic or body senses were probably most important in establishing the vertical, which was indicated by aligning the visual index with the main body axis." In other words, under these



circumstances the judgment became in essence merely the determination of the morphological vertical.

These findings become significant when one considers the design of an optimal experimental procedure for detecting changes in otolith function in the weightless environment. One cannot select a response that varies little, if at all, between the terrestrial and weightless environments as an indicator. The available data fortunately indicate that there are suitable indicator responses, such as changes in elevation of the morphological dead ahead plane, which will reflect the potential influence of changes in acceleration.

## GENERAL DISCUSSION

The subjective estimate of horizon data of Experiment I are in essential agreement with those of Schöne (9) which indicated that the visual perception of the direction of a force field for various static head tilts in the sagittal plane was altered when the intensity of the force field was varied even though no change occurred in the true morphological direction of the field. From his data, Schöne postulated that the horizon response was due exclusively to a force stimulus acting in the shear direction relative to the sensory epithelium located in the utricular cavity. He also postulated, in the form of a linear sine equation, that the horizon measure was linearly related or directly proportional to this shear-directed force. However, the horizon data of this study, collected over a wider stimulus range, do not confirm either of these points.

Similarly, the subjective estimate of vertical data of this study are in essential agreement with the investigations of Schöne (9), Colenbrander (1), and Miller and Graybiel (7) in which altering the intensity of the force field acting in the frontal head plane was found to introduce erroneous judgments of the true morphological direction of the field. Woellner and Graybiel (11) and Colenbrander (1) have studied the effects of frontal plane stimulation on the ocular counterroll response using the centrifuge to produce variable magnitude-variable direction stimuli. Woellner and Graybiel postulated a qualitative equation to relate the response linearly to a "lateral" shear-directed force. Though Colenbrander did not present a direct analysis of his counterroll data as a function of the shear force, he did reach the conclusion from his data and his subjective estimate of vertical data that such responses were directly proportional to the shear force component of his stimulus. The validity of this hypothesis for the frontal plane response is also questioned and will be discussed separately.

## THE VALIDITY OF A LINEAR SINE EQUATION FOR THE PREDICTION OF OTOLITH-RELATED RESPONSES

Schöne's linear sine equation was derived in part from the anatomical location of the receptor null axes obtained from his response data, the axes being those along which changes in the intensity of the acceleration had no effect on the subject's perception of

- the orientation of the force environment. For visual perception of vertical, minimal errors in response occurred only when the head was in the erect posture ( $\phi_x = 0$ ) relative to the direction of the force environment; static tilts of the head in the frontal plane to either side resulted in estimates of vertical with increased error whenever the intensity of the field was increased. For visual perception of horizon, minimal errors occurred only when the head was pitched approximately 30 degrees forward from the erect posture relative to the direction of the force environment; static pitches to either side of this 30-degree inclination of the sagittal plane of the head resulted in estimates of horizon with increased error whenever the intensity of the field was increased. Thus a common null point for the subjective vertical and horizon measures is found when the head is in an erect posture and pitched 30 degrees forward relative to the direction of the field. Schöne assumed that these data defined a common axis which was directed at right angles to the anatomical plane of the sensory epithelium of the utricular otolith mechanism. In effect, the data null points were used to locate the sensory epithelium of the utricle in a horizontal plane of the head which was tilted back approximately 25 to 30 degrees from the cardinal  $xy$  head plane, a location which in itself has some anatomical substantiation.

#### Sagittal Plane Stimulus: Subjective Horizon Response

Schöne resolved his static resultant acceleration stimulus into a component parallel to the hypothesized otolith receptor plane, i.e., the force in the shear direction, and a component acting perpendicular to the plane, i.e., the force in the compression direction. He then plotted his subjective estimate of horizon data as a function of the shear force and obtained an excellent straight-line fit. He concluded that the perceived horizon changes were effected exclusively by forces acting in the shear direction. That is, Schöne resolved the resultant of the gravitational and centripetal accelerations acting on the otolith receptor into "a pressure or pull component acting perpendicular to the sensory epithelium, and a shear component acting parallel to it. The shear is given by the product  $m \cdot f \cdot \sin \alpha$ , that is, the mass of the statolith ( $m$ ) times the strength of the mechanical field ( $f$ ) times the sine of the angle of inclination ( $\alpha$ ) the angle by which the animal or the organ in question is tilted out of zero position. Since the mass of the statolith remains constant, the shear changes proportional to  $f \cdot \sin \alpha$ ." From the straight-line fit afforded by his data, Schöne further postulated, in the form of a linear sine equation function, that the response was directly proportional to the magnitude of the shear force.

To facilitate visualization of these various parameters, the pertinent anatomical head axes and related stimuli are summarized in the sagittal view of the head presented in Figure 17. The  $x_o$  axis shown tilted upwards from the cardinal  $x$  head axis and the intersecting orthogonal  $y$  head axis defines Schöne's hypothesized plane of the sensory epithelium. In the remainder of the discussion, this plane will be identified as the "otolith plane"; the axis  $z_o$ , at right angles to this plane and which when aligned with the force field produces no change in perception of horizon when the field intensity is varied, will be identified as the "otolith null axis"; the component of the resultant

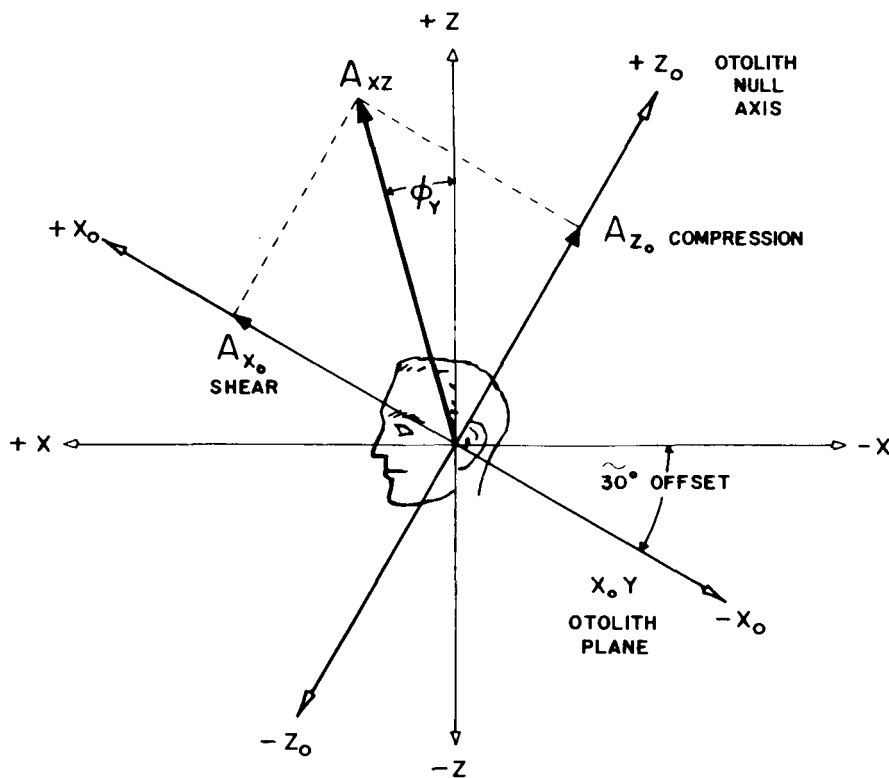


Figure 17

The anatomical head axes and related head stimuli in the sagittal plane stimulus configuration.

acceleration acting parallel to the otolith plane in the direction of the  $x_o$  axis will be identified as  $A_{x_o}$  and will be referred to as the "shear acceleration"; the component of the resultant acceleration acting along the  $z_o$  otolith null axis will be identified as  $A_{z_o}$  and be referred to as the "compression acceleration".

A plot of Schöne's horizon data (estimated from Figure 8, page 767, reference 9) as a function of the  $A_{x_o}$  shear acceleration is presented in Figure 18 where it is obvious that a relatively linear correspondence exists between the recorded  $\tau_y$  response and the hypothesized stimulus. (The diagonally drawn dashed line shown in this figure is presented only as a convenient slope reference and is not intended to provide a best straight-line fit of the data. In each subsequent graph which involves the plot of the  $\tau$  response as a function of the shear-directed stimulus, a corresponding line, of identical  $60^\circ/g$  slope, is drawn to facilitate the direct comparison of data collected by various investigators.) Schöne's data were collected from pitch forward inclinations of the sagittal plane of the head relative to the force field. By applying the same analysis to the data of the present study, collected for pitch backward as well as pitch forward inclinations, it would be expected that the same linear relationship would exist if Schöne's linear sine equation hypothesis were valid; i.e., incremental changes in the  $A_{x_o}$  shear acceleration should produce linearly proportional changes in the visual perception of horizon which are independent of the absolute value of  $A_{x_o}$ . More importantly, it is a fundamental point that if the response is to be attributed exclusively as

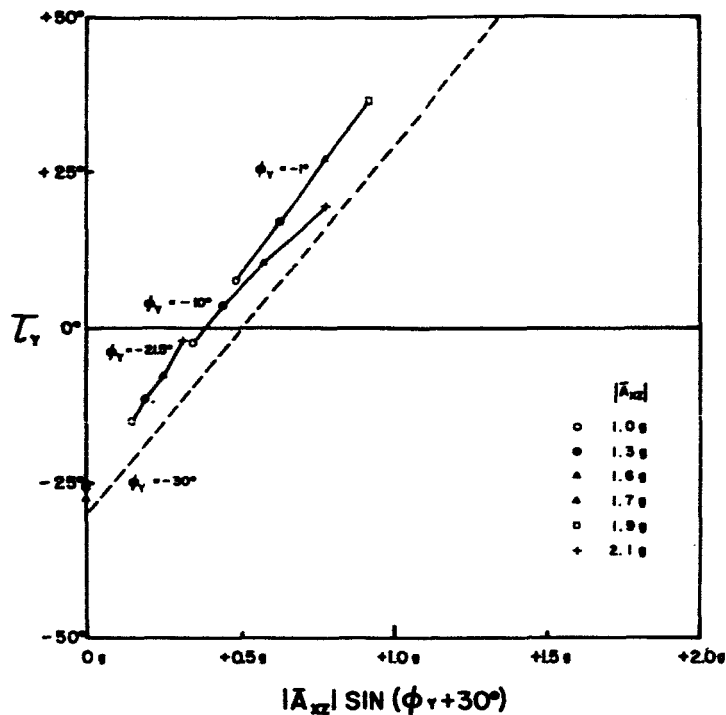


Figure 18

Subjective height of horizon data of Schöne: The response measure, expressed as  $\tau_y$ , is shown plotted as a function of the shear-directed component  $A_{x_0} = |\bar{A}_{xx}| \sin(\phi_y + 30^\circ)$  of the  $\bar{A}_{xx}$  sagittal plane acceleration stimulus. The diagonal dashed line is presented as a slope reference line to facilitate direct comparison of the various  $\tau_y$  and  $\tau_x$  plots as a function of the shear.

Schöne did (9, p 768) to a shear force, all stimulus configurations which produce identical shear forces should produce identical subjective horizon responses.

A plot of the  $\tau_y$  data of Experiment I as a function of the  $A_{x_0}$  shear acceleration for each stimulus condition is presented in Figure 19. Examination of this figure indicates that the horizon response is not a linear function of the shear force; i.e., incremental changes in the  $A_{x_0}$  stimulus do not produce directly proportional incremental changes in perception of the horizon over the stimulus range of the experiment. At most, the  $\tau_y$  measure was found to be a linear function of the stimulus for only the pitch forward inclinations of the head where the shear-directed accelerations fell into the 0.0 g to 0.5 g range. For the pitch backward inclinations of the head, not included in Schöne's work (9), pronounced nonlinearities existed. In effect, the incremental changes in visual perception of horizon became smaller and smaller as the shear-directed acceleration stimulus was raised above the 0.5 g level. The hypothesis that the visual perception of horizon is directly proportional to the shear-directed acceleration must be rejected.

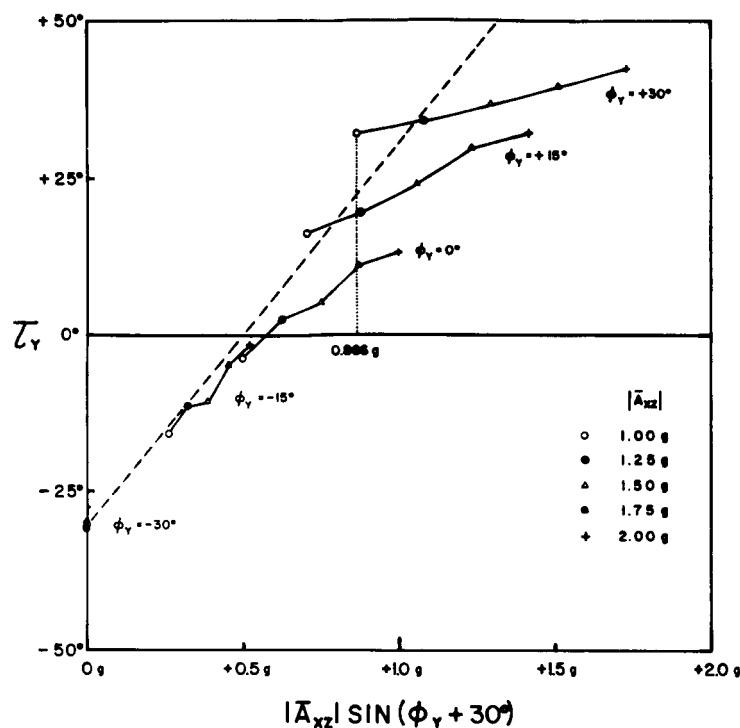


Figure 19

Subjective horizon data of present study: The response measure, expressed as  $\tau_y$ , is shown plotted as a function of the shear-directed component  $A_{x_0} = |\bar{A}_{xz}| \sin(\phi_y + 30^\circ)$  of the  $\bar{A}_{xz}$  sagittal plane acceleration stimulus. Note that identical values of the shear-directed stimulus do not produce identical subjective estimates of horizon as typified by the vertical dotted line drawn at  $A_x = 0.866 g$ .

Of greater importance, gross discontinuities in the  $\tau_y$  response data arose when the shear-directed accelerations were raised above the  $0.5 g$  level. In the present experiment three different chair-tilt-resultant acceleration combinations resulted in the application of near identical acceleration stimuli of about  $0.866 g$  in the shear direction. These combinations were described by a  $30^\circ$  pitch backward inclination in a  $1.00 g$  environment, a  $15^\circ$  pitch backward inclination in a  $1.25 g$  environment, and  $0^\circ$  tilt in a  $1.75 g$  field. This common  $0.866 g$  level is denoted by the vertical dotted line in Figure 19. As would be predicted for the  $30^\circ$  tilt in the terrestrial field, the  $\tau_y$  data indicate a relatively accurate estimation of the  $30^\circ$  depression of the force horizon. However, for the  $15^\circ$  tilt at  $1.25 g$  and  $0^\circ$  tilt at  $1.75 g$  configurations, the horizon was perceived at  $19^\circ$  and  $10^\circ$ , respectively, even though the shear acceleration stimulus had the same  $0.866 g$  value in each of the three cases.

The potential that other components of the stimulus could be responsible for the  $\tau_y$  changes observed when the primary shear-directed acceleration was held constant in magnitude can be investigated by referring to the family of graphs shown at the left of Figure 20 where the three axial acceleration components of concern are separately plotted against the resultant acceleration  $\bar{A}_{xz}$  for each  $\phi_y$  chair tilt angle:  $A_{x_0}$  is the primary shear acceleration assumed to produce variations in the subjective horizon;  $A_y$

# ACCELERATIONS ALONG THEORETICAL RECEPTOR AXES

SUBJECT SEATED RADIALLY FACING AXIS OF ROTATION

SUBJECT SEATED TANGENTIALLY WITH BACK TO DIRECTION OF ROTATION

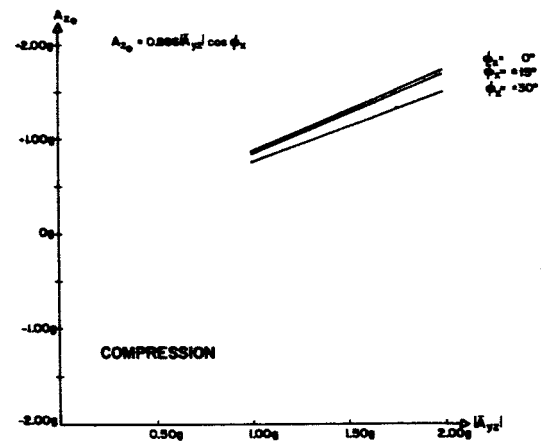
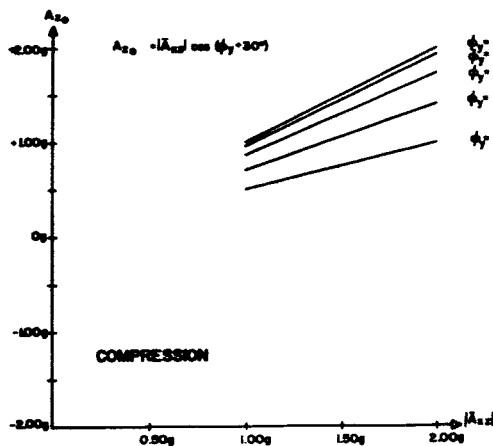
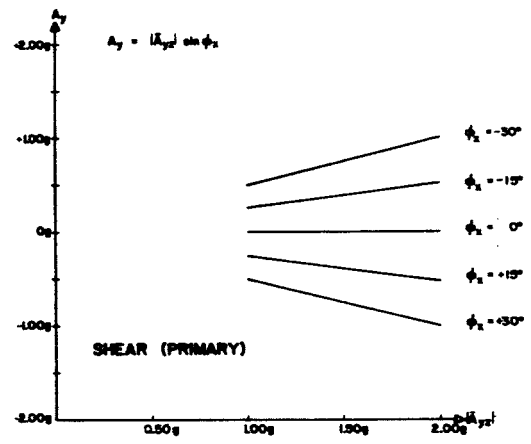
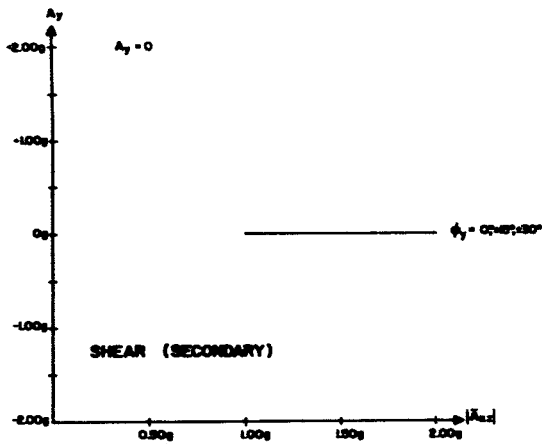
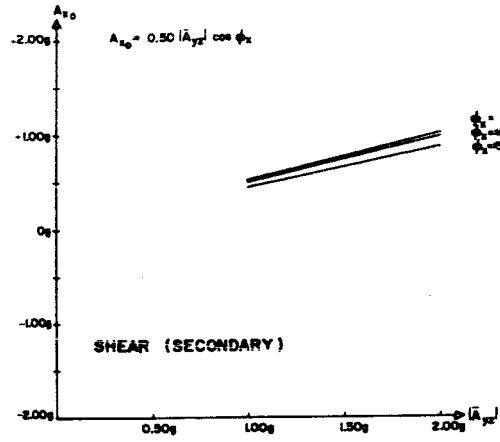
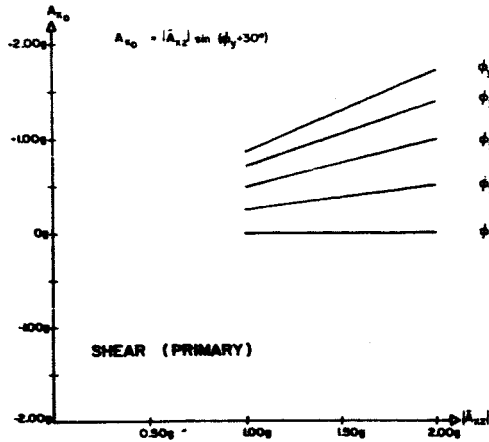


Figure 20

Magnitude of the  $A_{x_0}$ ,  $A_y$ , and  $A_{z_0}$  acceleration components acting along the theoretical receptor axes for the various magnitude and direction parameters of the resultant acceleration stimulus configurations used in the present study. The components for the radial and tangential orientations of the subjects are shown at the left and right, respectively. Note that for the tangential orientation, all components vary as the resultant stimulus changes in magnitude.

is the shear acceleration assumed to produce variations in the subjective vertical which was zero magnitude for the radial orientation of the subjects; and  $A_{z_0}$  is the acceleration acting along the  $z_0$  axis in the assumed compression direction. It may be immediately established that though the stimulus configurations of the previous paragraph resulted in near identical shear stimuli of approximately  $0.866 g$ , variations did occur in the  $A_{z_0}$  compression component. In effect, as the compression was raised from a  $0.5 g$  level in the  $+30^\circ$  at  $1.00 g$  condition to a  $1.5 g$  level in the  $0^\circ$  at  $1.75 g$  condition, the subjective horizon measure decreased nearly  $20^\circ$ . A plot of  $\tau_y$  as a function of  $A_{z_0}$  for the three constant magnitude  $A_{x_0} = 0.866 g$  stimulus configurations are shown at the left in Figure 21. Thus a condition exists where magnitude variations of the compression-directed component of the force field produce changes in the response even though no magnitude changes occur in the shear component.

Conversely, three stimulus configurations,  $0^\circ$  at  $1.00 g$ ,  $+15^\circ$  at  $1.25 g$ , and  $+30^\circ$  at  $1.75 g$ , lead to a condition where magnitude variations occur in the  $A_{x_0}$  shear acceleration with the  $A_{z_0}$  compression component held constant at approximately  $0.866 g$ . A plot of the accompanying variations of the subjective horizon as a function of the shear directed  $A_{x_0}$  acceleration is shown at the right in Figure 21. Thus the condition obtains where magnitude variations in the shear-directed component of the force field produce changes in the response even though no changes occur in the magnitude of the compression component.

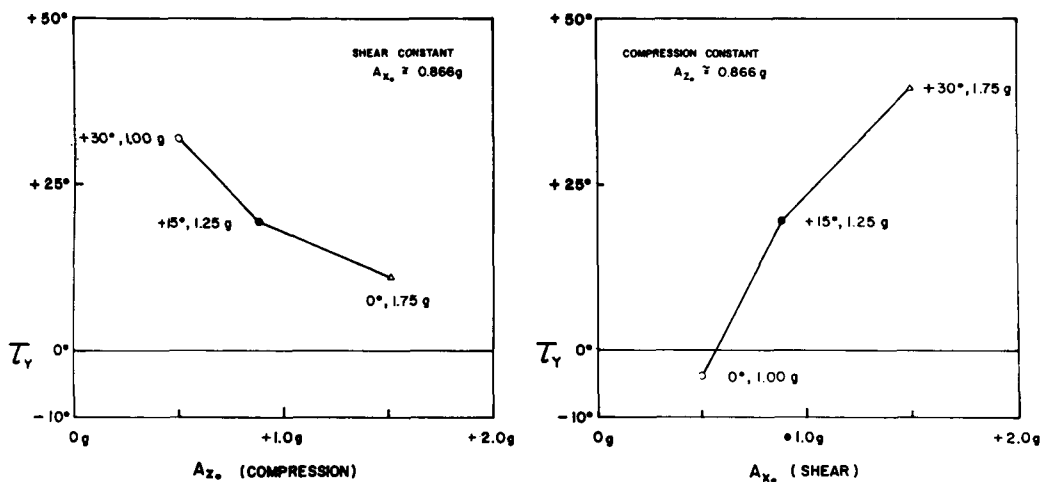


Figure 21

Selected subjective horizon data of present study plotted as a function of the shear-directed component of the stimulus with the compression-directed component held constant (right) and as a function of the compression-directed component with the shear component held constant (left). Note that both conditions produce changes in the subjective perception of horizon.

These discontinuities in the response for identical measures of the critical stimulus parameter likewise negate the hypothesis that the subjective perception of horizon capability is due singularly and exclusively to shear-directed accelerations. It is not, however, the intent of this statement to offer an argument against the shear concept of

otolith function. It is the intent to state that factors other than the shear accelerations must be introduced into any quantitative relationship postulated between a causal otolith force stimulus and an effected visual perception of horizon response.

Conclusions relative to horizon data of Figure 19 can be summarized at this point as follows:

1. When the otolith null axis,  $z_o$ , is aligned with the direction of a force field, the subjective visual perception of horizon will not be altered by changes in magnitude of the field, which is in complete agreement with Schöne and arrives from our data collected at the  $\phi_y = -30^\circ$  chair tilt angles. The implication is that when man is in an erect posture with the horizontal  $xy$  head plane inclined approximately  $30^\circ$  forward relative to the force field, his subjective perception of the force horizon,  $\tau_y = -30^\circ$ , will be independent of the intensity of the field.
2. When the otolith null axis  $z_o$  is tilted away from this alignment such that the orientation of the sagittal head plane is altered relative to the direction of the force field, changes in the perception of horizon will result. For such tilts an increase in the magnitude of the force field above the  $1.0 g$  gravitational level will result in an increase in error of estimation of the true direction of the resultant force horizon.
3. The changes in subjective perception of horizon arising from force stimuli of variable magnitude and direction are not a linear function of the shear-directed  $A_{x_o}$  acceleration component. Mathematically, a straight-line fit between  $\tau_y$  and  $|\bar{A}_{x_z}| \sin(\phi_y + 30^\circ)$  does not result. At most, a linear relationship arrives when  $A_{x_o}$  is less than  $0.5 g$ .
4. Identical  $A_{x_o}$  shear acceleration stimuli do not produce identical subjective estimates of horizon, indicating that factors other than  $A_{x_o}$  must be considered if a definitive system transfer function for the over-all otolith system is to be developed. These factors may derive from other components of the stimulus proper, or from the characteristics of the otolith system itself.
5. Stimulus configurations can be found where magnitude variations of the compression-directed  $A_{z_o}$  component of the field produce changes in the subjective perception of horizon even though the magnitude of the shear-directed  $A_{x_o}$  component is held fixed. The converse statement also applies.



## Frontal Plane Stimulus: Subjective Vertical/Ocular Counterroll Responses

It is usually assumed that the subjective perception of horizon and subjective perception of vertical response measures have a common origin in an otolith sensing system, or systems, with two degrees of freedom so that left-right as well as fore-aft head tilts can be simultaneously detected. Changes in perception of horizon arise from changes in direction of the force field acting in the sagittal  $xz$  head plane; changes in perception of vertical as well as ocular counterroll arise from changes in direction of the force field acting in the frontal  $yz$  head plane. With this assumption, it would then be expected that the conclusions reached from the response data for sagittal plane stimulation should have their counterparts in the response data arising from frontal plane stimulation.

To initiate this inquiry, the component of the resultant acceleration acting along the  $y$  head axis, i.e., the shear direction of the otolith plane for frontal plane tilts of the head, was calculated for each stimulus configuration of the present study and identified as  $A_y$ . A plot of the  $\tau_x$  subjective vertical data of Experiment I as a function of this  $A_y$  shear acceleration is presented in Figure 22 where  $A_y = |\bar{A}_{xz}| \sin \phi_x$ . The dashed diagonal slope reference line is drawn through the  $\tau_x = 0^\circ$ ,  $A_y = 0g$  and  $\tau_x = 30^\circ$ ,  $A_y = 0.5g$  coordinates. As with the horizon data, it is apparent that a linear relationship does not exist between the  $\tau_x$  response and the  $A_y$  stimulus acting

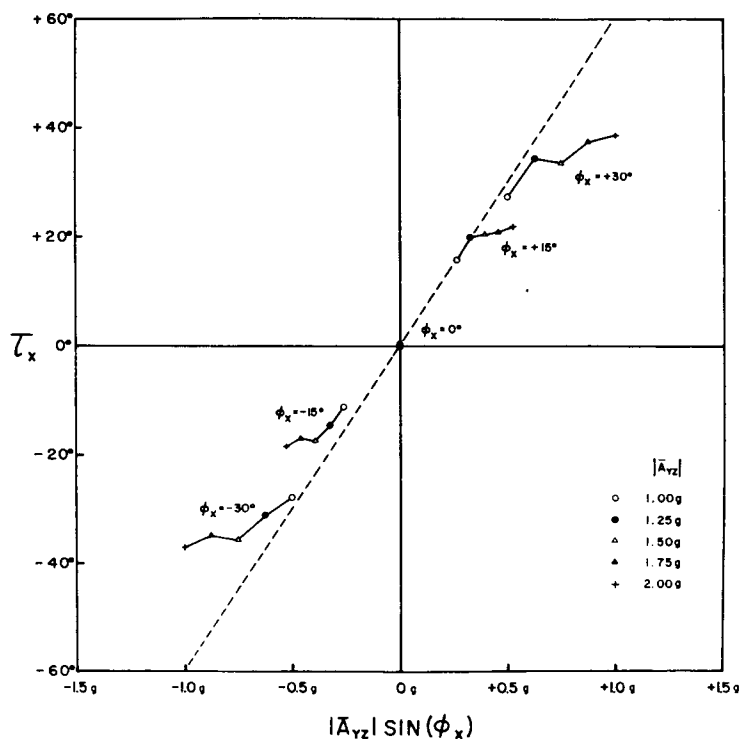


Figure 22

Subjective vertical data of present study: The response measure, expressed as  $\tau_x$ , is shown plotted as a function of the shear-directed component  $A_y = |\bar{A}_{yz}| \sin \phi_x$  of the  $\bar{A}_{yz}$  frontal plane acceleration stimulus.

in the shear direction; i.e., the change in  $\tau_y$  occurring when  $A_y$  is raised from 0.0  $g$  to 0.5  $g$  is much greater than that arising when  $A_y$  is raised from 0.5  $g$  to 1.0  $g$ . It also may be observed that the potential for discontinuities exists above the  $\pm 0.5 g$  shear acceleration levels although the effect is not so pronounced as observed with the horizon data. This could be explained in part by the observation that with the 30-degree pitch forward inclination of the hypothesized otolith receptor plane, it was possible to vary the  $A_x$  shear acceleration over the 0.0  $g$  to 1.75  $g$  range while for the tangential orientation it was possible to vary the  $A_y$  shear acceleration over a more limited 0.0  $g$  to 1.0  $g$  range in either direction.

A similar analysis was performed on the centrifuge data obtained on eight subjects by Miller and Graybiel in their investigation of the effect of magnitude and direction variations of frontal plane stimuli on the visual perception of subjective horizontal. This response measure is the equivalent of the  $\tau_x$  measure of this study in the context that the objective target alignments are complementary. In their study five different resultant acceleration stimuli,  $|A_{yz}| = 1.0, 1.2, 1.4, 1.6, 1.8$ , and  $2.0 g$ , and nine different body tilt angles,  $\phi_x = 0^\circ, \pm 10^\circ, \pm 20^\circ, \pm 30^\circ$ , and  $\pm 40^\circ$ , served to describe the frontal plane stimulus. In the analysis of the related data, the acceleration  $A_y$  acting along the  $y$  head axis in the hypothesized shear direction of the receptor was calculated for each stimulus configuration. Their response data (extracted from Figure 1, page 5, reference 7) was converted to the  $\tau_x$  notation of this study and then plotted as a function of the calculated shear stimulus.

The distribution of the data, shown in Figure 23, offers further evidence to support the present contention that the subjective vertical judgment is not a linear function of a shear-directed acceleration. The dashed diagonal line drawn through  $\tau_x = -30^\circ$ ,  $A_y = -0.5 g$  and  $\tau_x = +30^\circ$ ,  $A_y = +0.5 g$  coordinates for slope reference purposes allows one to observe the increasing nonlinearity between the pure shear force and the related response measure at the higher acceleration levels. In addition, the tendency for discontinuities to exist in the response for identical shear stimuli observed with our data is also present in their data as may be observed at the  $A_y = \pm 0.65 g$  level.

The same analytical procedure was used to evaluate Colenbrander's subjective visual perception of vertical data (1) obtained from a single subject on a centrifuge by tilt of the head relative to the torso. His sagittal plane stimuli were defined by three acceleration levels,  $|\bar{A}_{yz}| = 1.0, 1.5$ , and  $2.0 g$ , and nine different neck tilt angles,  $\phi_x = 0^\circ, \pm 15^\circ, \pm 30^\circ, \pm 45^\circ$ , and  $\pm 60^\circ$ . A plot of his data (averaged from the individual data points shown in Figure 17, page 77, reference 1 and converted to the present notation) as a function of the  $A_y$  shear acceleration is presented in Figure 24. Again the subjective estimate of vertical is a nonlinear function of  $A_y$  losing its effectiveness to influence  $\tau_x$  at the higher acceleration levels. Further, for these data there is no question of the potential for discontinuities in  $\tau_x$  for identical  $A_y$  shear stimuli.

Though Schöne (9) did not plot his subjective perception of vertical data as a function of the shear-directed stimulus, convincing support for the nonlinear hypothesis also

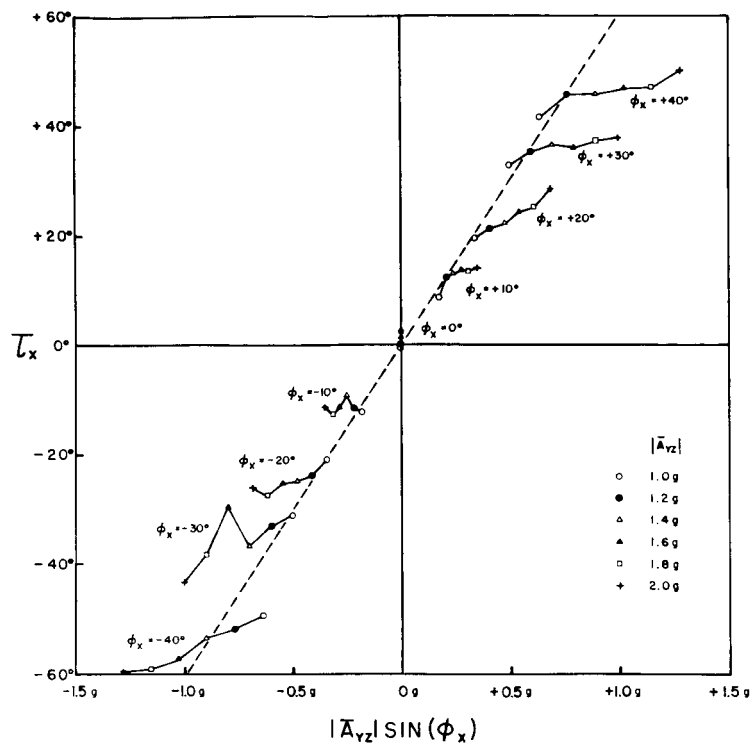


Figure 23

Egocentric visual localization of the horizontal data of Miller and Graybiel: The response measure, expressed as  $\tau_x$ , is shown plotted as a function of the shear-directed component  $A_y = |\bar{A}_{yz}| \sin \phi_x$  of the  $\bar{A}_{yz}$  frontal plane acceleration stimulus.

arrives from these data. These data, collected from a single subject and arrived at with a near 90-degree pitch backward neck tilt, involved two different acceleration levels,  $|\bar{A}_{yz}| = 1.0$  and  $2.0 g$ , and a selected series of leftward directed body tilt angles over the  $\phi_x = 0$  to  $180^\circ$  ranges. A plot of these data over the  $0^\circ < \phi_x < 90^\circ$  quadrant (estimated from Figure 4, page 765, reference 9) as a function of the calculated  $A_y$  shear acceleration is presented in Figure 25. Comparison of the slope of the data with the slope reference line readily establishes the nonlinearity of the response. A change of  $A_y$  from 0 to  $0.5 g$  produces a  $\tau_x$  variation of approximately  $25^\circ$ ; a change of  $A_y$  from  $1.0$  to  $2.0 g$  at the  $\phi_x = 60^\circ$  tilt produces a  $\tau_x$  change of less than  $20^\circ$  even though the change in stimulus magnitude is twice that of the first case. Further, this figure also displays the potential for discontinuities between  $\tau_x$  and identical magnitude shear stimuli.

It should be noted that when the otolith null axis is used as a stimulus reference rather than the cardinal  $x$ ,  $y$ , and  $z$  head axes, the  $\tau_x$  and  $\tau_y$  measures are not collected under identical stimulus conditions for the head erect posture. For the radial posture, the resultant acceleration was directed in the sagittal  $xz$  plane exclusively so that the secondary  $A_y$  shear acceleration was always zero as depicted at the left in Figure 20. With the subject seated tangentially with the stimulus directed in the frontal  $yz$  plane, the  $A_{x_0}$  shear-directed acceleration along the  $x_0$  axis as well as the main  $A_y$  shear

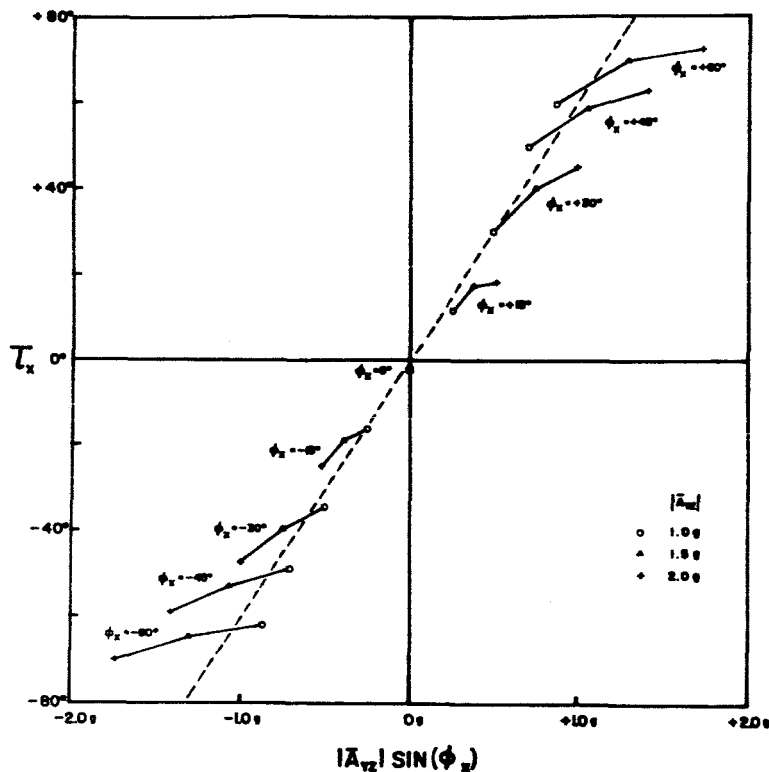


Figure 24

Subjective plumb line data of Colenbrander: The response measure, expressed as  $\tau_x$ , is shown plotted as a function of the shear-directed component  $A_y = |\bar{A}_{yz}| \sin \phi_y$  of the  $\bar{A}_{yz}$  frontal plane acceleration stimulus.

acceleration varied for each stimulus condition as depicted at the right in Figure 20. That is, the otolith plane, assumed to be tipped back approximately 30 degrees in the head, was never at right angles to the resultant. Discrepancies between the over-all trend of the  $\tau_x$  and  $\tau_y$  measures can then be investigated from the differential stimuli viewpoint.

Conclusions of the effect of frontal plane stimulation on the visual perception of vertical as derived from all these data can be summarized at this point as follows:

6. When the  $z$  head axis is aligned with the direction of a force field, the subjective visual perception of vertical will not be altered by changes in magnitude of the field. Note that this conclusion utilizes the  $z$  head axis as reference while its counterpart for the sagittal plane, Conclusion 1, utilizes the  $z_0$  otolith null axis as reference. This derives from the condition that in the erect posture for the radial orientation, the  $z_0$  axis was aligned with, or tilted relative to, the force field.

7. When the  $z$  head axis, or the  $z_0$  otolith null axis, is tilted away from this alignment so that the orientation of the frontal head plane is altered relative to the direction of the force field, changes in the visual perception of vertical occur. For such tilts, an increase in magnitude of the

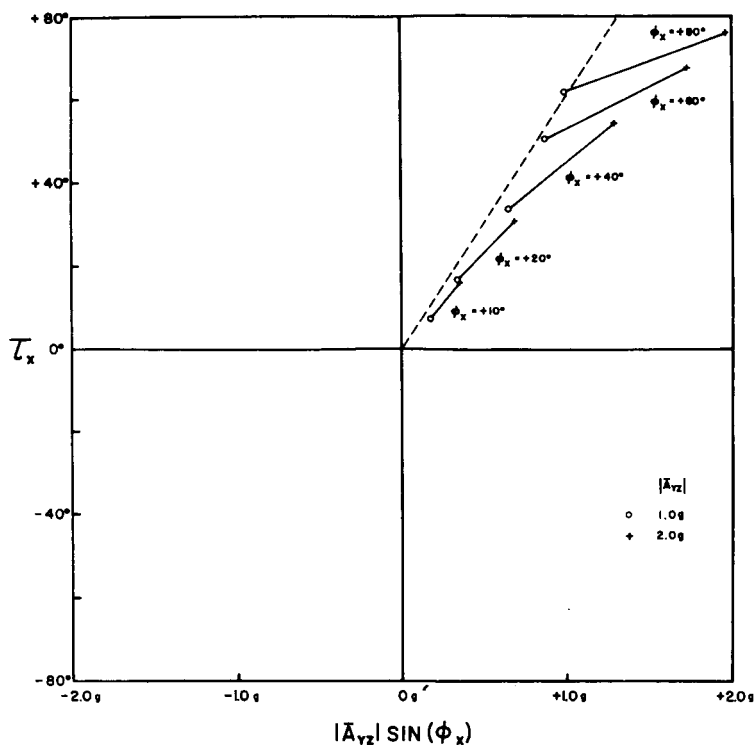


Figure 25

Subjective vertical data of Schöne: The response measure, expressed as  $\tau_x$ , is shown plotted as a function of the shear-directed component  $A_y = |\bar{A}_{yz}| \sin \phi_x$  of the  $\bar{A}_{yz}$  frontal plane acceleration stimulus.

force field above the 1.0  $g$  gravitational level will result in an increase of  $\tau_y$  in a direction representing an overestimation of the true angular direction of the resultant vertical.

8. The changes in subjective perception of vertical arising from force stimuli of variable magnitude and direction are not a linear function of the shear-directed  $A_y$  acceleration. Mathematically a straight line fit between  $\tau_x$  and  $|\bar{A}_{yz}| \sin \phi_x$  does not result. At most, a linear relationship arrives when  $A_y$  is less than 0.5  $g$ .

9. Identical  $A_y$  shear acceleration stimuli do not produce identical subjective estimates of vertical though the discontinuities of the  $\tau_x$  data are not so pronounced as those observed for the  $\tau_y$  data.

Although not detailed in this paper, when the same analytical procedures were performed on ocular counterroll data, the same form of nonlinearities was observed. Woellner and Graybiel (11), using photographs of the eye with anatomical references established by silk sutures introduced into the conjunctiva, measured counterroll for various head tilts made in the normal 1.0  $g$  environment as well as aboard the centrifuge. In their plot of these data against the  $A_y$  shear-directed stimulus (Figure 2, page 8,

reference 11) it may be observed that the slope of the ocular torsion measure as a function of the stimulus decreases at the higher acceleration levels. Similarly, counterroll data collected by Miller and Graybiel (6) using a precision photographic technique on nine normal subjects while exposed to various body tilts in the normal  $1.0 g$  field show the same nonlinearities. When these data (extracted from Table II, page 5, reference 6) are plotted against  $A_y$ , a linear relationship arises at most only over the  $0 < A_y < 0.5 g$  range. In fact, as they observed, the extent of the counterroll reached a maximum near a tilt of  $50^\circ$  ( $A_y \cong 0.766 g$ ) and in most cases tended to reverse in direction above this tilt. A degree of opposition to the nonlinearity concept, however, is provided by the counterroll data of Miller's study (5) on a single subject in a  $1.0 g$  environment. When these data (estimated from Figure 8, page 16, reference 5) are plotted against  $A_y$ , an excellent straight-line fit results between  $0 < A_y < 0.95 g$  for a rightward tilt. However, for the leftward tilt, values of  $A_y > 0.5 g$  lead to pronounced nonlinearities.

Colenbrander, using a blind-spot technique to measure the counterroll of each eye on a single subject while presenting stimuli of variable magnitude and direction in the sagittal plane, concluded from his data that the ocular torsion response was directly proportional to the shearing force of the otolith along its macula. However, when his data are plotted against  $A_y$ , the slope of the counterroll measure for  $A_y$  values near zero is greater than the slope for much greater values of  $A_y$ . These data also offer some conflict to those of Miller and Graybiel (6) which indicate that nonlinearities exist even in a  $1.0 g$  environment, much less the  $1.5$  and  $2.0 g$  force fields of the Colenbrander study. These variations may be attributable in part to the neck reflex complications discussed by Colenbrander since it was necessary that he achieve variations of stimulus direction through a tilt of the head relative to the torso as a result of the physical restrictions imposed by his centrifuge.

From these analyses of counterroll data, it is concluded that

10. Ocular counterroll is not a linear function of the  $A_y$  shear acceleration over the  $0 < A_y < 1 g$  stimulus range.

#### A TANGENT EQUATION FOR THE PREDICTION OF OTOLITH-RELATED RESPONSES

It has been shown that the subjective horizon and subjective vertical response measures, each assumed to arise from the same otolith system or systems, have the common property of not being linearly proportional to the so-called shear acceleration and of exhibiting discontinuities of the response parameter for identical values of the shear acceleration hypothesized to be the critical stimulus. Since, by mathematical definition, any function, linear or nonlinear, is automatically invalidated as a sufficient description if it can be shown to exhibit such discontinuities, any predictive equation based exclusively on response to shear must be incorrect.

Assuming the validity of the cited experimental data, the problem then becomes one of deriving a predictive equation which will relate both the magnitude and direction parameters of the force field to the  $\tau_y$  estimate of horizon data without introducing discontinuities. As was noted in the earlier analysis of the failure of equations based on sine functions to predict response in force environments other than the normal gravitational one, the so-called compression force could not be neglected as a significant component. Adopting the concept that compression force could at least affect the response, and possibly even effect it by acting in concert with the shear force, various analyses were performed on the data. It was found that the product of the relative intensity  $A$  of the field and the ratio of the shear-directed acceleration  $A_{x_0}$  to the compression-directed acceleration  $A_{z_0}$ , i.e.,  $A(A_{x_0} / A_{z_0})$ , or the shear acceleration modified by the cosine of the  $\varphi$  direction angle, i.e.,  $A_{x_0} / \cos \varphi$ , gave identical fits without significant discontinuities. Inspection revealed that both expressions were equivalent to  $A \sin \varphi / \cos \varphi$ , or, more simply,  $A \tan \varphi$ . Significantly, these expressions bear a direct relation to the  $\cotan \alpha$  function found by von Holst (4) in his experiments on fish wherein the visual stimulus was allowed to follow Lambert's cosine law of illumination.

This function when made specific for the subjective horizon data becomes  $|\bar{A}_{xz}| \tan (\varphi_y + 30^\circ)$  for the sagittal plane. The value of this function was calculated for each of the five chair tilt angles and each of the five acceleration magnitudes  $|\bar{A}_{xz}|$  of Experiment I. A plot of the related  $\tau_y$  subjective horizon data versus this function for all of the stimulus configurations is presented in Figure 26. It can be immediately realized that the discontinuities observed in Figure 19 when the  $\tau_y$  data were plotted as a function of only the  $A_{x_0}$  shear stimulus are virtually nonexistent with this tangent function.

For example, when the subject is in an erect posture ( $\varphi_y = 0^\circ$ ) in a 1.0  $g$  environment, the  $|\bar{A}_{xz}| \tan (\varphi_y + 30^\circ)$  function has a numerical value of 0.566. A nearly identical value obtains at a  $15^\circ$  forward head pitch ( $\varphi_y = -15^\circ$ ) in a 2.0  $g$  environment. As can be seen,  $\tau_y = -3^\circ$  and  $-1^\circ$ , respectively, for these two stimulus conditions. At the high end of the function, similar function values of about 1.7 are obtained for a  $30^\circ$  pitch backward inclination in a 1.0  $g$  field and a  $15^\circ$  backward tilt in a 1.75  $g$  field, with comparable  $\tau_y$  values of  $31.9^\circ$  and  $29.4^\circ$ , respectively.

It may also be observed that the response remains nonlinear; that is, increasing values of  $A \tan \varphi$  lead to correspondingly smaller changes in the perception of horizon. However, the general form of this nonlinearity is readily described by functions of trigonometric or equivalent form. For example, the arc tangent function provides an excellent conversion leading to an over-all response equation which not only predicts the trend of the data but well quantifies the absolute numerical value of the data. This particular conversion is described by the equation

$$\tau_y = \arctan \left[ |\bar{A}_{xz}| \tan (\varphi_y + 30^\circ) \right] - 30^\circ$$

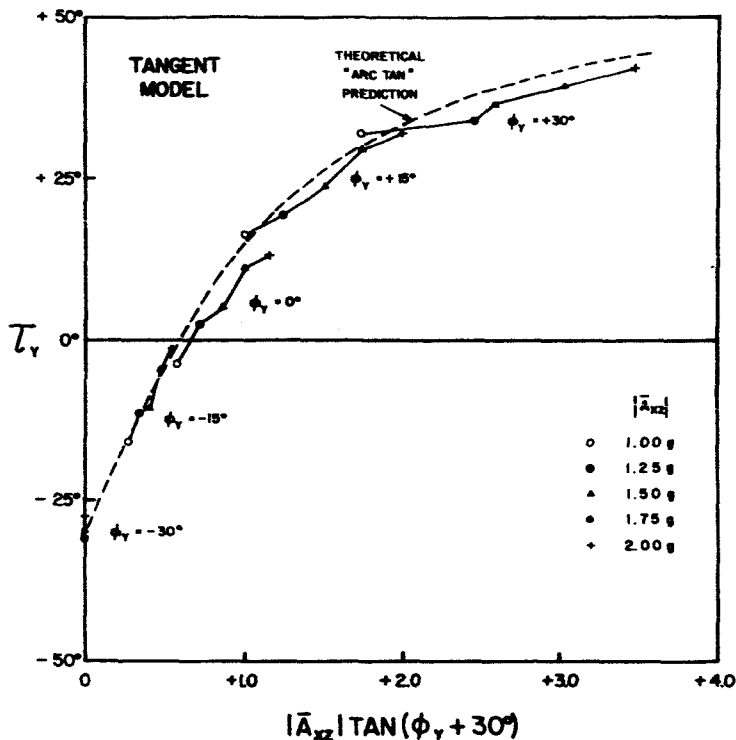


Figure 26

Subjective horizon data of present study: The response measure, expressed as  $\tau_y$ , is shown plotted against the sagittal plane tangent function  $|\bar{A}_{xz}| \tan(\phi_y + 30^\circ)$ . The dashed curve represents the theoretical response prediction of the "arc tan" conversion of the tangent function.

The value of this theoretical response equation was calculated for the various stimulus configurations and is shown plotted as a dashed line curve in Figure 26. With this particular arc tangent conversion, it obtains that the response equation in its basic form

$$\tau = \arctan A \tan \phi$$

is equivalent to the expression

$$\tan \tau = A \tan \phi$$

which if plotted for the various stimulus configurations would lead to a linear straight-line fit of the data.

Correspondingly, the  $A \tan \phi$  function becomes specific for the frontal plane stimulus when expressed as  $|\bar{A}_{yz}| \tan \phi_x$ . Plots of the  $\tau_x$  data derived from the present study and the studies of Miller and Graybiel, Colenbrander, and Schöne are presented in Figures 27, 28, 29, and 30, respectively. (The data of these figures are identical to those shown in Figures 22, 23, 24, and 25, respectively.) To facilitate comparison of all these data, the same arc tan conversion performed on the  $A \tan \phi$  function for the sagittal plane was performed on the corresponding function for this plane. This conversion, described by

$$\tau_x = \arctan |\bar{A}_{yz}| \tan \phi_x$$



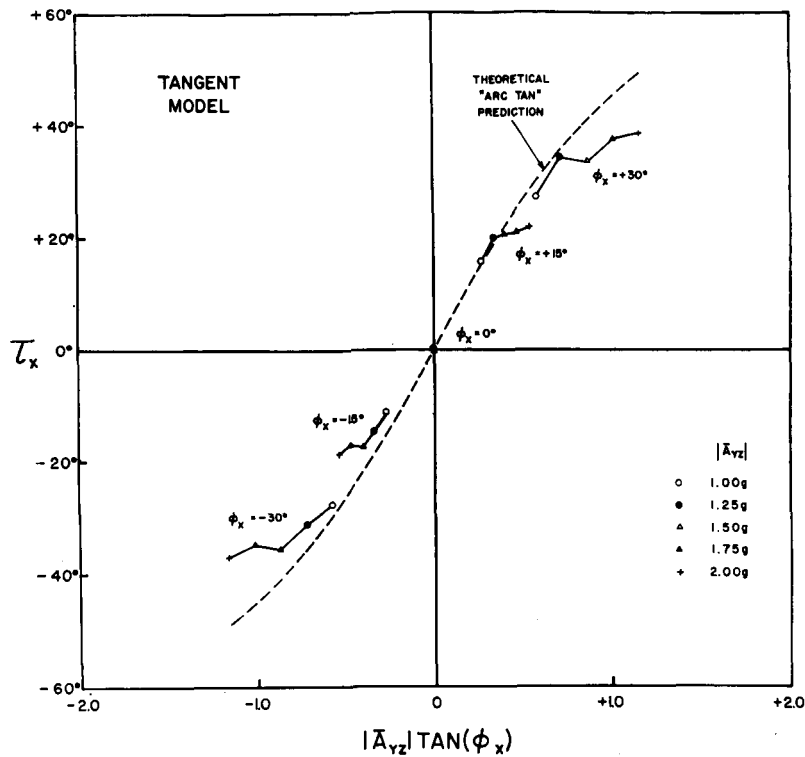


Figure 27

Subjective vertical data of present study: The response measure, expressed as  $\tau_x$ , is shown plotted against the frontal plane tangent function  $|\bar{A}_{yz}| \tan \phi_x$ .

is shown plotted as a dashed curve in each of these figures. As with the  $\tau_y$  data, the tangent equation well describes the trend of the  $\tau_x$  data although the same faithfulness of fit resulted only with Colenbrander's data. As discussed earlier, these variations can be related to the existence of slightly different stimulus conditions for the  $\tau_y$  and  $\tau_x$  judgments as denoted in Figure 20. It should be noted that no attempt was made to modify the arc tan conversion so as to obtain an even better fit for each set of data.

The tangent function offers a quantitative statement of the fact that supragravitational level force fields,  $A > 1.0 g$ , will effect an increase (in the Müller direction) in the subjective perception of the morphological orientation of a force field. For subgravitational level force fields,  $A < 1.0 g$ , the tangent equation postulates that the subjective measures will result in an underestimation (in the Aubert direction) of the true angular direction of the field, and provides a quantitative prediction of the extent of the response variations. It is obvious that in the true weightless condition of zero  $g$ , the equation has no direct significance since its components depend on a definition of the  $\phi$  measure of tilt which in itself is not existent, neither mathematically nor biologically, in a forceless environment. However, the findings indicate that the otolith masses will be in the same position of equilibrium as that established by the head erect ( $\phi_x = 0^\circ$ ,  $\phi_y = -30^\circ$ ) posture in the normal gravitational field.

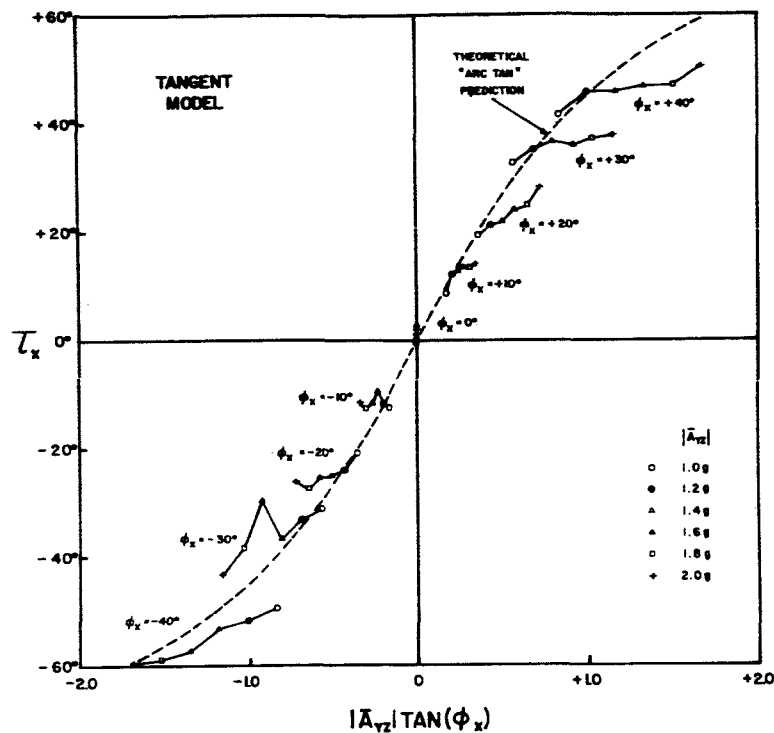


Figure 28

Egocentric visual localization of the horizontal data of Miller and Graybiel: The response measure, expressed as  $\tau_x$ , is shown plotted against the frontal plane tangent function  $|\bar{A}_{yz}| \tan \phi_x$ .

At the present stage of conceptual development the basic mechanics of the otolith system based on the previously cited conclusions and the  $A \tan \phi$  equation may be stated as follows: When man is in a posture where his  $z_0$  otolith null axis is aligned with the direction of his force environment, the otolith membrane is in a physiological null position. However, when the  $z_0$  otolith null axis is tilted away from this alignment with the resultant force field, the otolith membrane is displaced to a new position. Then the driving force, which is a function of the weight and tilt of the membrane, is in equilibrium with the restoring force, which is a function of the elastic properties of the otolith suspension system, whose stiffness varies with tilt. For a given tilt, increase in the magnitude of the force field produces an increase in the weight of the otolith membrane which results in a further displacement of the membrane from its physiological null position and a consequent overestimation of subjective horizon or vertical; decreases in the magnitude of the force field result in a decrease in the weight of the membrane which allows the elastic suspension system to return the membrane toward its physiological null position, with a consequent underestimation of subjective horizon or vertical. When exposed statically to a weightless environment, the otolith membrane will be in its physiological null position corresponding to the head erect posture in the normal terrestrial environment.

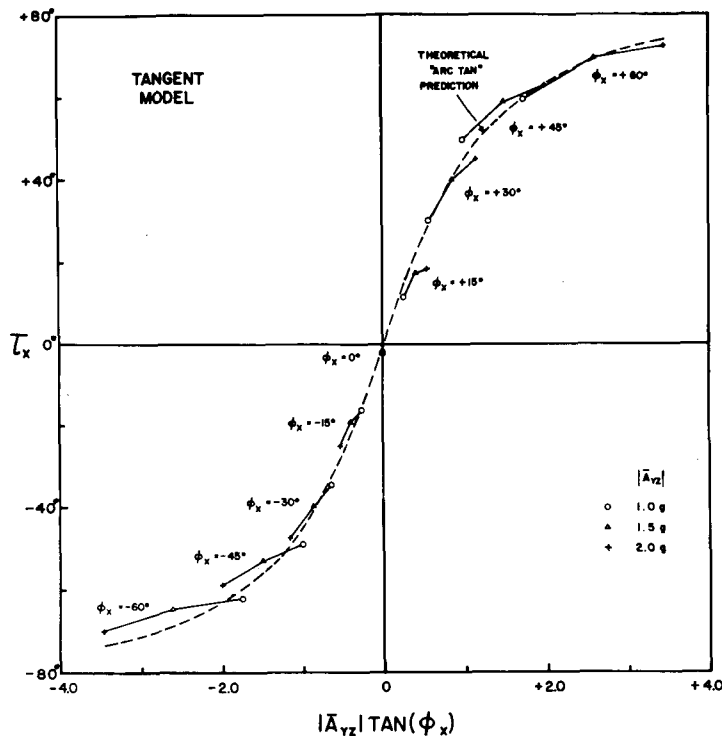


Figure 29

Subjective plumb line data of Colenbrander: The response measure, expressed as  $\tau_x$ , is shown plotted against the frontal plane tangent function  $|\bar{A}_{yz}| \tan \phi_x$ .

To summarize, the finding of this  $A \tan \phi$  function is significant in itself in that it is a mathematical expression which allows a quantitative prediction of the subjective visual perception of orientation which will be encountered under various stimulus conditions. It is not denied that the displacement of the otolith membrane from its null position may be linearly related to  $A \sin \phi$ , the shear-directed component of the static linear acceleration stimulus. Indeed, the  $A \tan \phi$  function can be readily interpreted to include this term by treating  $\cos \phi$  as a modifying factor contingent only upon the orientation of the individual. In effect, a definitive predictive equation for the response will probably involve the physical or neurological characteristics of the otolith system or even the contribution of other sensing systems, e.g., tactile, as well as the stimulus proper. Specifically, the tangent expression relates the  $\tau$  responses to the over-all transduction processes, which are directly related to the magnitude and direction elements of the stimulus and, as such, can be precisely measured and quantified. Based on the preceding discussion, the  $A \tan \phi$  function permits the following conclusions:

11. The discontinuities evident between the experimental data for estimation of horizon and vertical when linearly related to the  $A \sin \phi$  function are minimized when interpreted in terms of the  $A \tan \phi$  function.

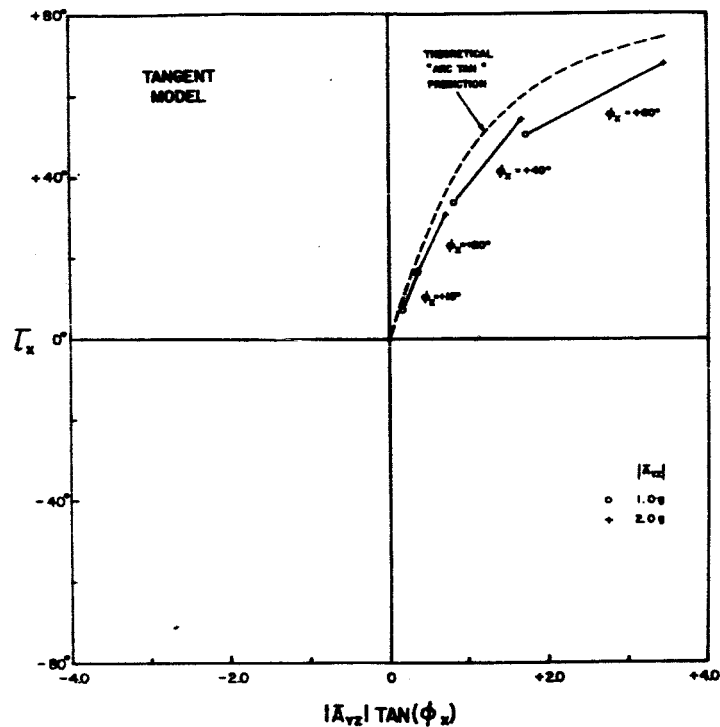


Figure 30

Subjective vertical data of Schöne: The response measure, expressed as  $\tau_x$ , is shown plotted against the frontal plane tangent function  $|\bar{A}_{vz}| \tan \phi_x$ .

12. The arc tan conversion of  $A \tan \phi$  well describes the nonlinear trend of the subjective vertical and horizon data.

13. The over-all tangent equation  $\tau = \arctan A \tan \phi$  provides a quantified prediction of the perceived direction of a force field when the magnitude and direction parameters of the field are varied.

## REFERENCES

1. Colenbrander, A., Eye and otoliths. Aeromed. Acta, Soesterberg, 9:45-91, 1963-4.
2. Hammer, L. R., Perception of the visual vertical under reduced gravity. AMRL-TDR-62-55. Wright-Patterson AFB, Ohio: Aerospace Medical Research Laboratories, 1962.
3. Hixson, W. C., Instrumentation for the Pensacola Centrifuge-Slow Rotation Room I facility. NSAM-875. NASA Order R-37. Pensacola, Fla.: Naval School of Aviation Medicine, 1963.
4. Holst, E. von, Die Tätigkeit des Statolithenapparats im Wirbeltierlabyrinth. (The function of the statolith apparatus in the vertebrate labyrinth.) Naturw., 37:265-272, 1950.
5. Miller, E. F., II, Counterrolling of the human eyes produced by head tilt with respect to gravity. NSAM-833. NASA Order R-47. Pensacola, Fla.: Naval School of Aviation Medicine, 1962.
6. Miller, E. F., II, and Graybiel, A., A comparison of ocular counterrolling movements between normal persons and deaf subjects with bilateral labyrinthine defects. NSAM-838. NASA Order R-47. Pensacola, Fla.: Naval School of Aviation Medicine, 1962.
7. Miller, E. F., II, and Graybiel, A., Magnitude of gravito-inertial force, an independent variable in egocentric visual localization of the horizontal. NSAM-901. NASA Order R-47. Pensacola, Fla.: Naval School of Aviation Medicine, 1964.
8. Müller, G. E., Über das Aubertsche Phänomen. (Concerning the Aubert phenomenon.) Z. Psychol. Physiol. Sinnesorg., 49:109-244, 1916.
9. Schöne, H., On the role of gravity in human spatial orientation. Aerospace Med., 35:764-772, 1964.
10. Tschermak-Seysenegg, A. von (translated by Boeder, P.), Introduction to Physiological Optics. Springfield, Ill.: Charles C Thomas, 1952.
11. Woellner, R. C., and Graybiel, A., Counterrolling of the eyes and its dependence on the magnitude of gravitational or inertial force acting laterally on the body. J. appl. Physiol., 14:632-634, 1959.

**APPENDIX A**  
**Experimental Data**

Table A1

Mean Angular Displacement of the Apparent Horizon ( $\tau_y$ ) as a Function of the Magnitude ( $|\bar{A}_{xz}|$ ) and Direction ( $\phi_y$ ) of a Linear Acceleration Vector ( $\bar{A}_{xz}$ ) Acting in the  $xz$  Plane of the Body

		$ \bar{A}_{xz} $ (g units)									
Subject	$\phi_y$ (deg)	1.00		1.25		1.50		1.75		2.00	
		$\bar{X}$ (deg)	s (deg)	$\bar{X}$ (deg)	s (deg)	$\bar{X}$ (deg)	s (deg)	$\bar{X}$ (deg)	s (deg)	$\bar{X}$ (deg)	s (deg)
DCA	-30	-32.2	1.6	-34.1	1.2	-35.8	1.1	-33.7	1.4	-27.4	3.3
	-15	-19.5	0.6	-11.1	2.9	-12.7	0.4	-11.5	1.8	-11.2	2.1
	0	- 5.7	2.0	- 5.3	2.5	- 7.9	1.1	- 3.4	1.6	- 5.4	3.4
	+15	+14.0	2.4	+11.7	4.3	+19.2	1.8	+24.5	1.7	+28.3	2.5
	+30	+35.3	1.1	+24.2	1.4	+29.3	3.5	+33.0	1.2	+43.7	0.2
MJC	-30	-30.5	1.2	-28.6	1.0	-32.8	1.0	-31.1	1.0	-31.7	0.7
	-15	-11.0	0.4	- 7.5	0.7	- 4.9	0.8	+ 1.2	0.9	+ 4.3	0.6
	0	+ 3.6	1.8	+11.1	1.2	+14.0	0.8	+19.0	1.4	+23.1	1.8
	+15	+20.3	1.0	+27.0	1.3	+29.6	2.2	+33.9	1.9	+37.8	1.1
	+30	+37.8	1.7	+47.0	2.3	+47.4	1.4	+48.0	1.0	+47.4	1.1
JIN	-30	-27.6	2.3	-27.5	0.0	-27.4	2.7	-27.5	2.1	-24.4	1.9
	-15	-12.6	1.1	- 8.8	1.7	- 1.1	1.8	+ 1.2	2.6	+ 7.5	1.6
	0	- 2.1	1.3	+ 3.5	1.5	+10.3	1.9	+17.9	2.3	+24.7	4.4
	+15	+19.9	1.6	+24.5	3.2	+27.1	1.8	+37.3	2.3	+39.5	2.8
	+30	+27.8	2.7	+35.5	1.5	+36.2	1.5	+40.6	2.0	+43.7	3.2
AT	-30	-31.2	1.3	-34.9	1.3	-27.6	0.7	-26.5	0.9	-25.6	3.3
	-15	-19.7	1.7	-17.8	0.3	-13.3	1.6	- 9.8	1.2	- 5.7	1.3
	0	- 3.7	1.4	+ 0.3	0.2	+ 3.7	0.7	+10.5	0.5	+ 9.6	2.4
	+15	+10.6	1.4	+14.1	0.9	+19.4	1.0	+22.0	0.7	+21.8	0.5
	+30	+26.7	0.9	+28.7	1.5	+32.9	1.4	+35.9	1.3	+33.5	2.9
Group mean	-30	-30.4	1.6	-31.3	1.0	-30.9	1.6	-29.7	1.4	-27.3	2.5
	-15	-15.7	1.1	-11.3	1.7	- 8.0	1.3	- 4.7	1.7	- 1.3	2.2
	0	- 2.0	1.6	+ 2.4	1.6	+ 5.0	1.2	+11.0	1.7	+13.0	3.2
	+15	+16.2	1.7	+19.3	2.8	+23.8	1.8	+29.4	1.7	+31.9	2.4
	+30	+31.9	1.8	+33.9	1.7	+36.5	2.1	+39.4	1.4	+42.1	2.2

Table A2

Mean Angular Displacement of the Apparent Vertical ( $\tau_x$ ) as a Function of the Magnitude ( $|\bar{A}_{yz}|$ ) and Direction ( $\phi_x$ ) of a Linear Acceleration Vector ( $\bar{A}_{yz}$ ) Acting in the  $yz$  Plane of the Body

Subject $\phi_x$ (deg)		$ \bar{A}_{yz} $ ( $g$ units)									
		1.00		1.25		1.50		1.75		2.00	
		$\bar{X}$ (deg)	$s$ (deg)	$\bar{X}$ (deg)	$s$ (deg)	$\bar{X}$ (deg)	$s$ (deg)	$\bar{X}$ (deg)	$s$ (deg)	$\bar{X}$ (deg)	$s$ (deg)
DCA	-30	-27.7	0.6	-33.9	4.8	-37.4	5.2	-37.0	2.7	-36.3	4.7
	-15	- 8.3	0.9	-15.9	2.4	-19.8	2.4	-18.9	1.4	-24.7	2.8
	0	+ 0.9	0.6	- 0.3	0.7	- 0.3	0.7	- 1.0	0.8	- 0.3	1.0
	+15	+17.4	2.2	+22.2	1.3	+26.0	1.8	+21.5	2.1	+21.6	2.1
	+30	+26.5	0.3	+32.9	3.5	+28.7	3.3	+34.3	2.8	+35.2	1.3
MJC	-30	-26.6	0.9	-31.2	0.9	-38.9	1.3	-33.5	1.9	-38.1	2.0
	-15	-10.6	0.6	-14.5	1.0	-18.1	0.8	-17.8	0.3	-17.3	0.7
	0	+ 1.5	0.2	+ 4.4	1.0	+ 3.6	0.9	+ 3.3	1.4	+ 3.5	1.5
	+15	+18.8	1.0	+22.5	0.9	+23.7	1.6	+28.0	1.9	+30.1	1.6
	+30	+26.8	0.7	+36.0	1.5	+38.9	1.0	+41.3	2.1	+38.9	1.7
JIN	-30	-28.0	1.6	-31.4	0.9	-34.9	0.6	-36.4	1.5	-36.6	0.4
	-15	-12.4	0.6	-15.0	0.9	-16.9	1.1	-17.4	0.4	-18.1	0.3
	0	- 2.4	0.5	- 2.2	0.8	- 2.5	0.3	- 2.5	0.1	- 2.2	0.4
	+15	+12.5	1.2	+19.5	0.3	+18.8	0.9	+19.3	0.6	+21.3	0.7
	+30	+30.9	1.3	+40.9	3.4	+41.6	2.5	+46.7	3.6	+43.0	1.7
AT	-30	-28.8	0.4	-28.2	2.3	-30.9	1.1	-32.0	0.8	-36.4	2.0
	-15	-13.5	1.2	-12.6	0.5	-14.7	0.6	-13.9	1.3	-14.0	1.0
	0	- 0.2	1.0	- 0.1	0.8	- 1.2	0.7	- 2.0	0.5	- 1.3	0.6
	+15	+13.3	0.2	+14.9	0.8	+12.7	1.6	+14.0	1.5	+14.0	1.7
	+30	+24.6	0.9	+26.9	1.9	+24.2	1.2	+27.2	2.8	+37.3	3.1
Group mean	-30	-27.8	1.0	-31.2	2.7	-35.5	2.8	-34.7	1.8	-36.9	2.7
	-15	-11.2	0.9	-14.5	0.8	-17.4	1.4	-17.0	1.2	-18.5	1.6
	0	- 0.1	0.6	+ 0.5	0.8	- 0.1	0.7	- 0.6	0.8	- 0.1	1.0
	+15	+15.5	1.4	+19.8	0.9	+20.3	1.5	+20.7	1.6	+21.8	1.6
	+30	+27.2	0.9	+34.2	2.7	+33.4	2.2	+37.4	2.9	+38.6	2.1



Table A3

Mean Angular Displacement of Apparent Dead Ahead ( $\tau_y$ ) in the Vertical Dimension as a function of the Magnitude ( $|\bar{A}_{xz}|$ ) and Direction ( $\phi_y$ ) of a Linear Acceleration Vector ( $\bar{A}_{xz}$ ) Acting in the  $xz$  Plane of the Body

Subject	$\phi_y$ (deg)	$ \bar{A}_{xz} $ (g units)							
		1.00		1.25		1.50		1.75	
		$\bar{X}$ (deg)	s (deg)	$\bar{X}$ (deg)	s (deg)	$\bar{X}$ (deg)	s (deg)	$\bar{X}$ (deg)	s (deg)
MJC	-30	+0.9	0.6	+ 1.5	1.0	- 0.4	2.4	- 0.4	1.4
	-15	+0.2	2.0	+ 5.9	1.3	+ 3.2	3.0	- 5.9	0.6
	0	+3.1	2.3	+12.5	1.5	+11.9	2.8	+13.6	0.9
	+15	+3.2	1.8	+ 9.9	1.2	+10.0	1.2	+ 8.2	1.2
	+30	+3.1	1.8	+11.1	2.2	+12.6	0.8	+11.3	0.7
JIN	-30	-4.2	1.9	- 1.1	1.8	- 6.8	2.6	- 6.1	1.6
	-15	-4.6	1.2	- 3.2	1.1	- 2.1	0.8	- 0.9	1.5
	0	+1.1	1.6	+ 5.4	1.1	+ 7.2	1.2	+13.4	1.7
	+15	-1.1	1.7	+ 2.0	1.4	- 3.2	2.3	- 1.0	1.0
	+30	-1.3	1.9	+ 0.3	4.1	- 3.6	1.9	- 8.8	1.7
TLO	-30	-10.1	3.2	-13.6	3.5	-14.5	4.0	-17.5	1.3
	-15	-1.6	1.8	- 1.1	0.8	0.0	1.2	- 1.5	0.8
	0	-4.3	1.5	+ 0.1	0.4	+ 2.0	0.8	+ 4.2	0.8
	+15	-4.5	2.7	- 1.0	1.1	- 0.2	4.0	- 0.4	2.2
	+30	-3.7	1.1	- 7.2	1.2	- 2.5	0.9	- 7.8	2.4
TES	-30	+8.4	0.8	+ 0.1	2.3	+ 4.8	2.1	+ 6.8	4.7
	-15	-1.0	3.7	- 3.3	1.6	- 1.1	0.8	- 0.8	2.6
	0	+1.5	0.4	+ 7.9	1.6	+10.7	0.8	+12.1	1.7
	+15	+5.0	1.3	+ 3.6	3.1	+11.4	1.1	+11.8	1.1
	+30	+0.6	0.9	- 9.5	2.4	- 5.6	0.6	- 3.5	1.1
Group mean	-30	-1.3	1.9	- 3.3	2.3	- 4.2	2.9	- 4.3	2.7
	-15	-1.8	2.4	- 0.4	1.2	0.0	1.7	+ 0.7	1.6
	0	+0.4	2.3	+ 6.5	1.3	+ 8.0	1.6	+10.8	1.4
	+15	+0.7	1.9	+ 3.6	1.9	+ 4.5	2.5	+ 4.7	1.0
	+30	-0.3	1.5	+ 1.3	2.7	+ 0.2	1.1	- 2.2	1.6

Table A4

Mean Angular Displacement of Apparent Dead Ahead ( $\tau_z$ ) in the Horizontal Dimension as a Function of the Magnitude ( $|\bar{A}_{xz}|$ ) and Direction ( $\phi_y$ ) of a Linear Acceleration Vector ( $\bar{A}_{xz}$ ) Acting in the  $xz$  Plane of the Body

Subject	$\phi_y$ (deg)	$ \bar{A}_{xz} $ (g units)							
		1.00		1.25		1.50		1.75	
		$\bar{X}$ (deg)	$s$ (deg)	$\bar{X}$ (deg)	$s$ (deg)	$\bar{X}$ (deg)	$s$ (deg)	$\bar{X}$ (deg)	$s$ (deg)
MJC	-30	+1.2	0.6	+1.4	1.2	+0.2	0.8	0.0	0.3
	-15	+1.6	0.3	+0.4	1.0	+0.6	0.7	0.0	0.6
	0	-0.1	0.5	-1.7	0.8	-2.3	1.1	-2.3	0.9
	+15	+0.3	0.8	+0.1	0.9	-1.1	1.5	-1.1	1.5
	+30	+1.4	1.1	+0.1	0.5	+0.2	1.8	-1.2	1.1
JIN	-30	-1.3	0.9	-0.2	0.7	-0.6	1.2	-0.8	0.3
	-15	-1.0	1.7	-0.5	0.5	-0.9	1.6	-1.1	0.8
	0	-0.9	0.8	-0.4	0.8	-0.1	0.5	-1.7	0.2
	+15	-0.4	0.8	-0.6	0.4	-0.9	0.4	-0.8	1.0
	+30	-1.1	1.2	-0.9	1.4	+2.0	1.2	-0.8	1.2
TLO	-30	-4.1	1.0	-6.5	1.0	-5.6	1.0	-6.2	1.9
	-15	-3.1	1.2	-4.6	1.0	-3.9	0.8	-3.6	0.8
	0	-3.5	0.9	-3.8	0.8	-4.4	0.9	-6.2	0.9
	+15	-4.7	1.0	-4.7	0.8	-6.1	1.5	-7.5	0.3
	+30	-2.0	0.5	-3.5	1.5	-5.0	0.1	-5.6	1.5
TES	-30	+2.0	1.0	+2.4	0.8	+1.7	1.8	+2.1	2.3
	-15	+0.9	0.7	+2.3	0.9	+1.1	0.4	+0.7	0.9
	0	+1.6	1.6	+1.8	1.4	+0.8	1.5	-1.4	1.6
	+15	+2.8	0.9	+1.0	0.4	+0.6	1.2	+0.8	0.8
	+30	+1.4	0.2	+0.9	0.3	+0.6	0.4	+0.4	1.0
Group mean	-30	-0.6	0.9	-0.7	1.0	-1.1	1.2	-1.2	1.5
	-15	-0.4	0.8	-0.6	0.9	-0.8	1.0	-1.0	0.8
	0	-0.7	1.0	-1.0	1.0	-1.5	1.1	-2.9	1.0
	+15	-0.5	0.9	-1.1	0.7	-1.9	1.3	-2.2	1.0
	+30	-0.1	0.9	-0.9	1.1	-0.6	1.9	-1.8	1.2

Table A5

Mean Angular Displacement of Apparent Dead Ahead ( $\tau_y$ ) in the Vertical Dimension as a Function of the Magnitude ( $|\bar{A}_{yz}|$ ) and Direction  $\phi_y$  of a Linear Acceleration Vector ( $\bar{A}_{yz}$ ) Acting in the  $yz$  Plane of the Body

Subject	$\phi_y$ (deg)	$ \bar{A}_{yz} $ (g units)							
		1.00		1.25		1.50		1.75	
		$\bar{X}$ (deg)	s (deg)	$\bar{X}$ (deg)	s (deg)	$\bar{X}$ (deg)	s (deg)	$\bar{X}$ (deg)	s (deg)
MJC	-30	-0.6	1.1	- 2.0	1.6	+ 0.8	3.7	- 0.1	1.0
	-15	+1.0	1.3	+ 8.7	1.2	+ 8.3	1.2	+10.1	1.5
	0	+1.9	0.6	+ 6.1	1.0	+ 9.8	0.6	+10.1	1.0
	+15	-1.3	1.9	+ 3.3	2.0	+ 4.0	1.4	+ 1.5	2.3
	+30	-2.6	1.8	+ 1.8	1.4	+ 2.5	1.9	+ 5.7	1.7
JIN	-30	-2.8	1.6	- 0.4	1.9	+ 1.1	1.9	+ 5.5	1.3
	-15	-3.0	0.6	+ 0.2	1.1	+ 3.4	1.2	+ 6.1	2.1
	0	-1.6	0.9	+ 2.2	0.8	+ 7.4	1.2	+10.8	0.5
	+15	-7.5	1.9	- 7.8	2.5	- 7.9	0.5	- 4.8	0.5
	+30	-5.0	2.0	- 2.4	1.7	- 1.4	1.8	+ 2.6	2.9
TLO	-30	+4.5	1.3	+ 6.8	0.8	+12.7	3.6	+14.1	2.1
	-15	+2.8	1.0	+10.6	0.9	+13.5	3.0	+14.0	2.5
	0	+0.5	1.0	+ 9.0	2.0	+14.3	0.8	+18.9	2.1
	+15	+0.8	1.6	+ 8.3	1.5	+13.5	1.6	+16.9	0.4
	+30	+4.8	3.6	+15.8	1.9	+14.6	1.3	+13.6	1.5
TES	-30	-0.4	0.7	+ 7.4	1.4	+ 9.3	0.6	+10.7	0.7
	-15	+0.5	0.9	+ 5.6	2.2	+ 9.7	0.3	+ 9.7	0.9
	0	+3.0	0.9	+ 8.0	1.1	+12.9	0.8	+15.3	0.6
	+15	-0.2	0.5	+ 6.4	0.5	+ 6.7	3.5	+ 7.0	1.5
	+30	-2.4	2.0	+ 2.1	1.1	+ 0.7	0.0	+ 4.7	0.6
Group mean	-30	+0.2	1.2	+ 3.0	1.5	+ 6.0	1.1	+ 7.6	1.4
	-15	+0.3	1.0	+ 6.3	2.0	+ 8.7	1.8	+10.0	1.9
	0	+1.0	1.0	+ 6.3	1.3	+11.1	0.9	+13.8	1.3
	+15	-2.1	1.6	+ 2.6	1.8	+ 4.1	2.7	+ 5.2	1.4
	+30	-1.3	2.5	+ 4.3	1.6	+ 4.1	1.5	+ 6.7	1.9

Table A6

Mean Angular Displacement of Apparent Dead Ahead ( $\tau_z$ ) in the Horizontal Dimension as a Function of the Magnitude ( $|\bar{A}_{yz}|$ ) and Direction ( $\phi_x$ ) of a Linear Acceleration Vector ( $\bar{A}_{yz}$ ) Acting in the  $yz$  Plane of the Body

Subject	$\phi_x$ (deg)	$ \bar{A}_{yz} $ (g units)							
		1.00		1.25		1.50		1.75	
		$\bar{X}$ (deg)	$s$ (deg)	$\bar{X}$ (deg)	$s$ (deg)	$\bar{X}$ (deg)	$s$ (deg)	$\bar{X}$ (deg)	$s$ (deg)
MJC	-30	-0.5	1.0	+1.3	2.7	-0.4	3.9	-4.6	1.6
	-15	+2.8	0.6	-0.5	2.2	+1.4	1.3	+1.3	2.2
	0	+1.5	1.2	+3.0	2.4	+1.2	0.9	+2.0	1.4
	+15	+0.6	2.0	+1.9	1.9	-0.1	2.1	+1.0	1.2
	+30	+3.1	1.6	+6.6	2.4	+4.8	2.0	+5.2	3.4
JIN	-30	+1.0	2.5	+2.0	0.7	+0.7	1.9	+0.5	0.7
	-15	+0.9	2.1	+2.2	0.9	+3.1	1.9	+3.7	1.2
	0	+0.5	1.1	+0.5	1.5	-0.7	0.4	-0.1	0.9
	+15	+0.1	2.4	+2.9	2.3	+4.5	1.0	+0.8	1.2
	+30	-3.7	1.7	-0.5	1.3	-0.5	0.8	+0.6	1.0
TLO	-30	-0.3	0.9	+0.2	0.9	-1.4	0.8	-3.9	1.0
	-15	-1.7	0.5	-4.2	0.6	-5.6	0.8	-5.6	1.8
	0	-3.2	0.9	-5.0	1.3	-5.8	0.5	-7.0	0.9
	+15	-0.5	0.8	-0.7	1.1	-1.0	0.4	-3.0	0.7
	+30	-2.8	1.3	-2.5	1.1	-1.9	1.4	-2.1	1.3
TES	-30	+0.5	0.7	+1.8	1.7	+0.6	0.7	-1.6	0.9
	-15	+0.8	1.2	+1.5	1.3	+0.5	0.6	+2.0	1.1
	0	+2.6	1.0	+1.7	0.7	0.0	1.4	+0.8	0.8
	+15	+1.5	1.4	-0.6	1.5	0.0	0.4	+1.6	1.0
	+30	+0.2	1.5	+1.0	0.9	-0.5	0.2	+0.5	1.4
Group mean	-30	+0.2	1.5	+1.3	1.7	-0.1	2.2	-2.4	1.1
	-15	+0.7	1.3	-0.3	1.5	-0.2	1.3	+0.4	1.6
	0	+0.4	1.1	+0.1	1.6	-1.3	0.9	-1.1	1.0
	+15	+0.4	1.8	+0.9	1.8	+0.9	1.2	+0.1	1.0
	+30	-0.8	1.5	+1.2	1.6	+0.5	1.7	+1.1	2.0

Table A7

Mean Angular Displacement of Apparent  $z$  Body Axis ( $\tau_z$ ) as a Function of the Magnitude ( $|\bar{A}_{yz}|$ ) and Direction ( $\phi_z$ ) of a Linear Acceleration Vector ( $\bar{A}_{yz}$ ) Acting in the  $yz$  Plane of the Body

Subject	$\phi_z$ (deg)	$ \bar{A}_{yz} $ (g units)							
		1.00		1.25		1.50		1.75	
		$\bar{X}$ (deg)	$s$ (deg)	$\bar{X}$ (deg)	$s$ (deg)	$\bar{X}$ (deg)	$s$ (deg)	$\bar{X}$ (deg)	$s$ (deg)
MJC	-30	- 1.6	1.9	+ 2.0	1.1	0.0	2.4	+ 4.4	0.6
	0	- 0.3	1.0	- 1.4	1.1	+2.1	0.8	+ 2.8	0.7
	+30	- 6.9	1.2	- 4.8	0.8	-4.9	1.4	- 5.5	0.8
JIN	-30	+ 0.8	0.7	- 0.5	1.8	+ 1.8	1.1	+ 1.6	0.9
	0	-10.7	0.4	- 9.7	0.4	- 8.6	0.4	- 9.0	0.5
	+30	+ 6.8	2.1	+ 6.8	0.6	+ 5.3	1.2	+ 3.3	1.5
TLO	-30	- 4.1	0.8	- 7.0	2.1	- 5.6	1.4	- 4.4	1.4
	0	- 1.9	0.6	- 0.9	0.5	- 0.8	0.6	- 1.8	0.8
	+30	- 8.4	2.0	-11.7	2.2	-13.4	1.9	-11.7	2.5
TES	-30	- 1.6	2.7	0.0	5.2	- 0.5	3.1	+ 1.0	2.7
	0	-10.8	0.4	-10.6	0.5	-11.5	0.4	-12.0	0.1
	+30	- 2.6	2.5	- 8.8	1.1	- 5.3	1.7	- 8.5	2.2
Group mean	-30	- 1.6	1.8	- 1.4	3.0	- 1.1	2.2	+ 0.7	1.6
	0	- 5.9	0.6	- 5.7	0.7	- 4.7	0.6	- 5.0	0.6
	+30	- 2.8	2.0	- 4.6	1.4	- 4.6	1.6	-55.6	1.9

**APPENDIX B**  
**Statistical Analyses**

Table B1

Summary of Variance Analysis for Error of Adjustment of a Target to Horizon

Source	S.S.	d.f.	M.S.	F	p
Total	3835.14	19	201.85		
Between direction angles ( $\phi_y$ )	892.90	4	223.23	1.14	> .05
Between subjects	2942.24	15	196.15		
Total	6641.71	99	67.09		
Between magnitude   $\bar{A}_{xz}$   linear $\phi_y = -30^\circ$ error	1790.31 -	4 -	447.58 -	38.52	< .001
Linear $\phi_y = -15^\circ$ error	501.97 96.48	1 12	501.97 8.04	62.43	< .001
Linear $\phi_y = 0^\circ$ error	594.44 238.89	1 12	594.44 19.91	29.86	< .001
Linear $\phi_y = +15^\circ$ error	677.33 62.63	1 12	677.33 5.22	129.76	< .001
Linear $\phi_y = +30^\circ$ error	270.92 216.06	1 12	270.92 18.01	15.04	< .01
Magnitude   $\bar{A}_{xz}$   x Direction angle ( $\phi_y$ )	312.24	16	19.52	1.68	> .05
Within subjects	2806.57	80	35.08		
Remainder	697.02	60	11.62		

Table B2

## Summary of Variance Analysis for Error of Adjustment of a Target to Vertical

Source	S.S.	d.f.	M.S.	F	p
Total	1286.05	19	67.69		
Between direction angles ( $\phi_x$ )	348.79	4	87.20	1.40	> .05
Between subjects	937.26	15	62.48		
Total	2374.85	99	23.99		
Between magnitude $ \bar{A}_{yz} $	541.27	4	135.32	25.15	< .001
Linear $\phi_x = -30^\circ$	188.36	1	188.36		
error	46.39	12	3.87	48.67	< .001
Linear $\phi_x = -15^\circ$	117.65	1	117.65		
error	93.29	12	7.77	15.14	< .01
Linear $\phi_x = 0^\circ$	-	-	-		
error	-	-	-		
Linear $\phi_x = +15^\circ$	72.37	1	72.37		
error	73.82	12	6.15	11.77	< .01
Linear $\phi_x = +30^\circ$	270.40	1	270.40		
error	119.17	12	9.93	27.23	< .001
Magnitude $ \bar{A}_{yz} $ x Direction angle ( $\phi_x$ )	224.73	16	14.05	2.61	< .01
Within subjects	1088.80	80	13.61		
Remainder	322.80	60	5.38		



Table B3

Summary of Variance Analysis for Error of Vertical Adjustment of a Target to Dead Ahead

Source	S.S.	d.f.	M. S.	F	p
Total	478.72	19	25.20		
Between direction angles ( $\phi_y$ )	60.88	4	15.22	-	
Between subjects	418.84	15	27.86		
Total	532.34	79	6.74		
Between magnitude   $\bar{A}_{xz}$	12.47	3	4.16	6.82	< .001
Linear $\phi_y = -30^\circ$ error	-	-	-		
Linear $\phi_y = -15^\circ$ error	-	-	-		
Linear $\phi_y = 0^\circ$ error	216.48 19.41	1 9	216.48 2.16	100.22	< .001
Linear $\phi_y = +15^\circ$ error	-	-	-		
Linear $\phi_y = +30^\circ$ error	-	-	-		
Magnitude   $\bar{A}_{xz}$   x Direction angle ( $\phi_y$ )	13.91	12	1.16	1.90	> .05
Within subjects	53.62	60	0.89		
Remainder	27.24	45	0.61		

Table B7

Summary of Variance Analysis for Error of Adjustment of a Target to  $z$  Body Axis

Source	S.S.	d.f.	M.S.	F	p
Total	1249.37	11	113.58		
Between direction angles ( $\phi_x$ )	133.79	2	66.90	-	
Between subjects	1115.56	9	123.95		
Total	1349.81	47	28.72		
Between magnitude $ \bar{A}_{yz} $	3.42	3	1.14		
Linear $\phi_x = -30^\circ$ error	-	-	-		
Linear $\phi_x = -15^\circ$ error	-	-	-		
Linear $\phi_x = 0^\circ$ error	-	-	-		
Linear $\phi_x = +15^\circ$ error	-	-	-		
Linear $\phi_x = +30^\circ$ error	-	-	-		
Magnitude $ \bar{A}_{yz} $ x Direction angle ( $\phi_x$ )	17.81	6	2.97	1.01	> .05
Within subjects	100.44	36	2.79		
Remainder	79.21	27	2.93		

Table B6

Summary of Variance Analysis for Error of Horizontal Adjustment of a Target to Dead Ahead

Source	S. S.	d.f.	M. S.	F	p
Total	408.77	19	21.51		
Between direction angles ( $\phi_x$ )	13.44	4	3.36	-	
Between subjects	395.33	15	26.36		
Total	520.69	79	6.59		
Between magnitude $ \bar{A}_{yz} $	11.09	3	3.70	2.74	> .05
Linear $\phi_x = -30^\circ$ error	-	-	-		
Linear $\phi_x = -15^\circ$ error	-	-	-		
Linear $\phi_x = 0^\circ$ error	-	-	-		
Linear $\phi_x = +15^\circ$ error	-	-	-		
Linear $\phi_x = +30^\circ$ error	-	-	-		
Magnitude $ \bar{A}_{yz} $ x Direction angle ( $\phi_x$ )	39.92	12	3.33	2.47	< .05
Within subjects	111.92	60	1.87		
Remainder	60.91	45	1.35		

Table B4

Summary of Variance Analysis for Error of Horizontal Adjustment of a Target to Dead Ahead

Source	S. S.	d.f.	M. S.	F	p
Total	2998.35	19	157.81		
Between direction angles ( $\phi_y$ )	900.85	4	225.21	1.61	> .05
Between subjects	2097.50	15	139.83		
Total	3731.07	79	47.23		
Between magnitude $ \bar{A}_{xz} $	57.47	3	19.16	2.09	> .05
Linear $\phi_y = -30^\circ$ error	-	-	-		
Linear $\phi_y = -15^\circ$ error	-	-	-		
Linear $\phi_y = 0^\circ$ error	-	-	-		
Linear $\phi_y = +15^\circ$ error	-	-	-		
Linear $\phi_y = +30^\circ$ error	-	-	-		
Magnitude $ \bar{A}_{xz} $ x Direction angle ( $\phi_y$ )	262.45	12	21.87	2.38	< .05
Within subjects	732.72	60	12.21		
Remainder	412.80	45	9.17		

Table B5

Summary of Variance Analysis for Error of Vertical Adjustment of a Target to Dead Ahead

Source	S. S.	d.f.	M. S.	F	p
Total	761.46	19	40.08		
Between direction angles ( $\phi_x$ )	331.40	4	82.85	2.89	> .05
Between subjects	430.06	15	28.67		
Total	3084.35	79	39.04		
Between magnitude $ \bar{A}_{yz} $	913.86	3	304.62	10.29	< .001
Linear $\phi_x = -30^\circ$	126.76	1	126.76		
error	49.56	9	5.51	23.01	< .001
Linear $\phi_x = -15^\circ$	197.19	1	197.19		
error	13.91	9	1.55	127.22	< .001
Linear $\phi_x = 0^\circ$	374.11	1	374.11		
error	29.31	9	3.26	114.76	< .001
Linear $\phi_x = +15^\circ$	106.95	1	106.95		
error	85.77	9	9.53	11.22	< .01
Linear $\phi_x = +30^\circ$	114.48	1	114.48		
error	29.89	9	3.32	34.48	< .001
Magnitude $ \bar{A}_{yz} $ x Direction angle ( $\phi_x$ )	77.65	12	6.47		
Within subjects	2322.89	60	38.71		
Remainder	1331.38	45	29.59		

**APPENDIX C**  
**Description of Experimental Apparatus**

The Digital Angular Position Target assembly developed for the  $\tau_x$  measures of this study utilized a commercially available shaft position encoder (Theta Instrument Corporation, Model "Decitrak") to measure angular orientation of the target. With this encoder system, transduction of shaft angle to an analog electrical signal is accomplished by a rotary transmitter which contains internal coding discs fixed to a stationary housing. These discs, in conjunction with a rotating brush block assembly fixed to the rotary shaft of the transmitter, provide a four digit, 10 wire per digit, parallel output electrical identification of shaft angle. The coded transmitter signal is then routed to an electronic gate array module with internal logic networks to sequentially program the code into a nonambiguous decimal format suitable to drive a digital readout or printer. For this study, a lamp-bank type readout indicator installed in the Monitor Console displayed shaft position directly in degrees over the complete 0.000 to 359.9 degree range with an over-all accuracy of  $\pm 0.2$  degree.

Front and rear view photographs of the target assembly are shown at the left and right, respectively, of Figure C1. A view of the target with the aluminum enclosure, 8 inches in diameter and 8 inches deep, removed to show interior details is presented in Figure C2. The luminous target proper was attached to a bearing-supported shaft which was in-line connected to the shaft of the transmitter encoder via an Oldham coupling to minimize radial or axial loading of the transmitter. Rotation of the target was provided by a small capacitor type gear-reducer instrument motor which was gear-coupled to the target shaft. This motor (Bodine Electric Company, Series B8262E-1800) could be rotated in either direction, could be reversed electrically while rotating, and was rated to deliver a torque output of 110 inch-ounces at its 0.7 RPM output shaft speed which was adequate to supply the 20 inch-ounce breakaway torque requirements of the transmitter encoder. Dual sets of parallel wired microswitches at the subject and experimenter stations operated two relays mounted within the target housing that controlled the direction of motor rotation. Quick start and stop motions of the target were provided by normally closed relay contacts which shorted the motor capacitor to effect dynamic braking action.

The Linear Displacement Target assembly used for the  $\tau_y$  measure of target elevation or depression was derived from a modified slide-wire carriage assembly obtained from an electronic curve-follower type recorder (Electronic Associates Inc., Model 205L Variplotter). The carriage assembly consisted of a precision wire-wound slide-wire mechanism with a movable electrical contact arm that could be mechanically driven over the full 30-inch length of the slide wire. The contact arm was fixed to a continuous steel tape loop which was passed over bearing-supported pulley wheels mounted at opposite ends of the slide-wire mechanism. Motive power for the tape loop was provided by a small 10 RPM gear-reducer motor which was direct-coupled to the shaft of the lower pulley. Photographs of the target assembly with and without its outer protective housing are shown at the left and right, respectively, of Figure C3.

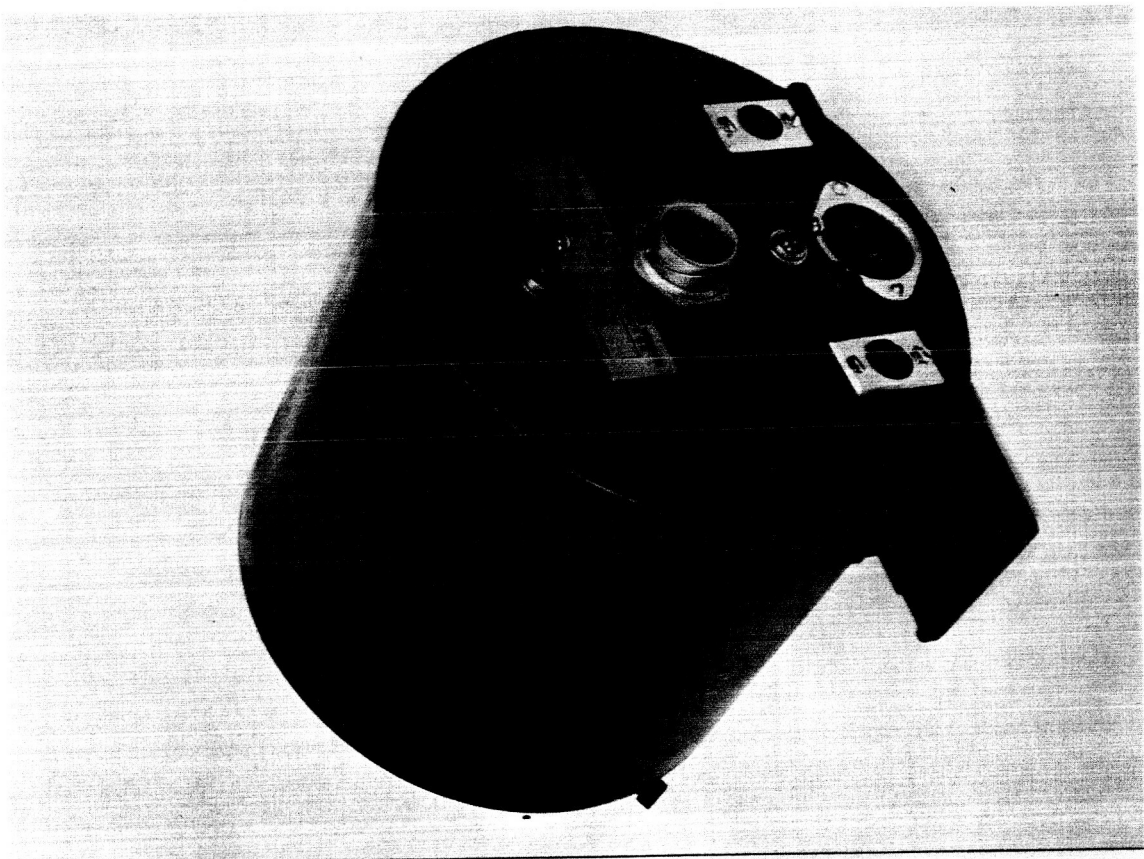
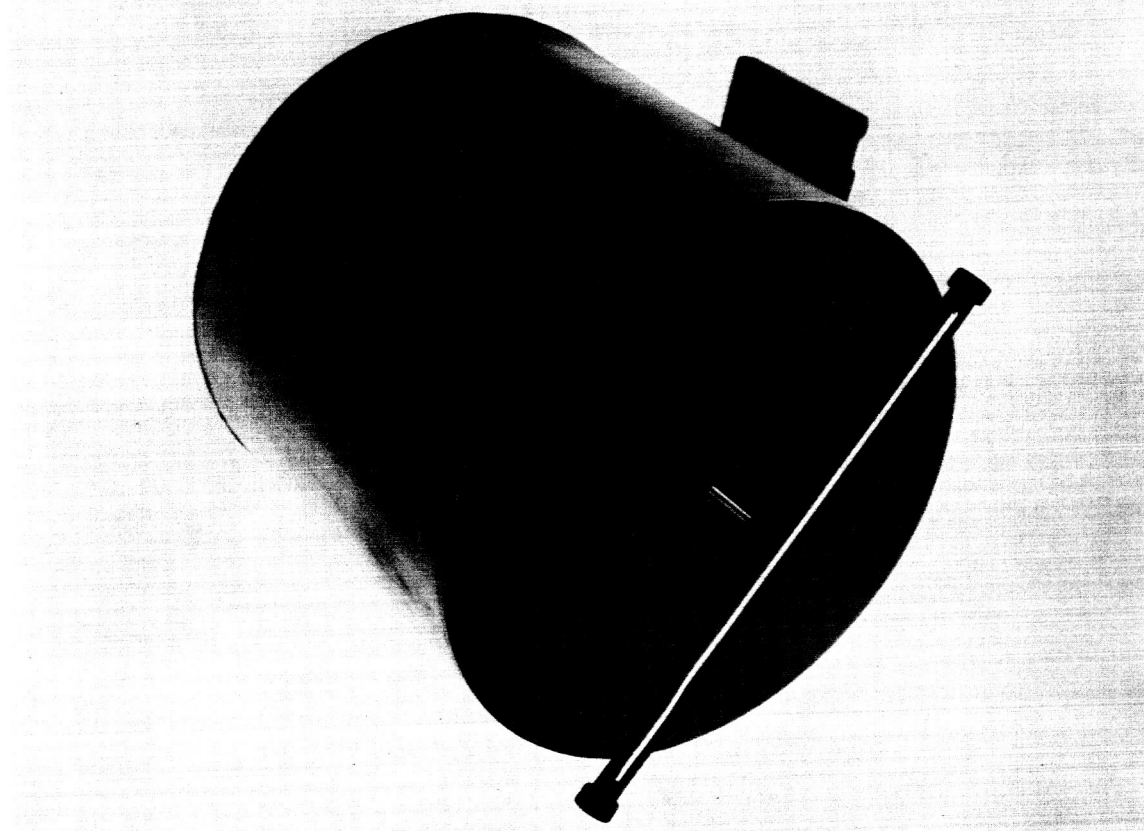


Figure C1

The Digital Angular Position Target used for the  $\tau_x$  response measures of this study as viewed from the front (left) and the rear (right).



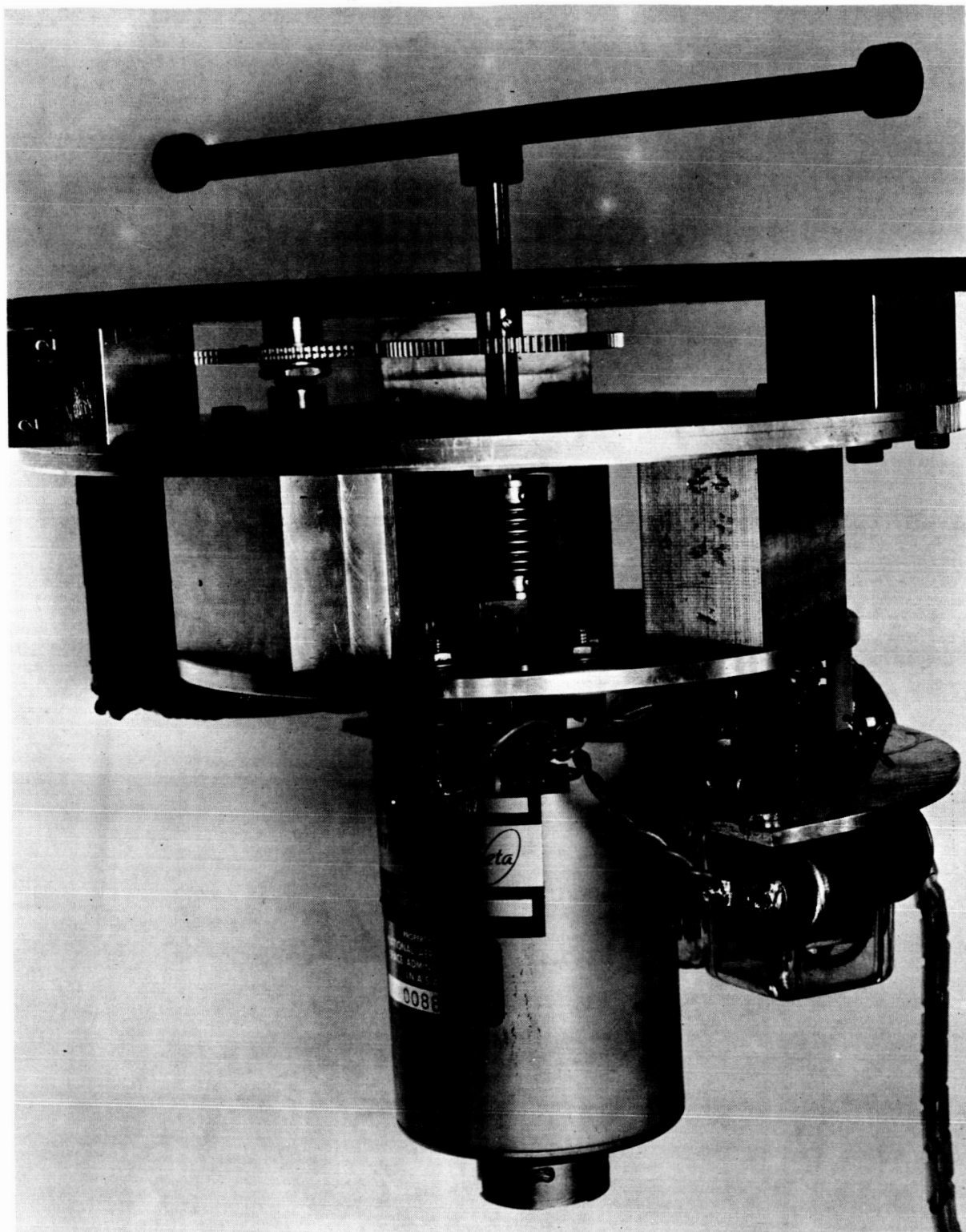


Figure C2

The Digital Angular Position Target with the outer housing removed to show the interior assembly details.

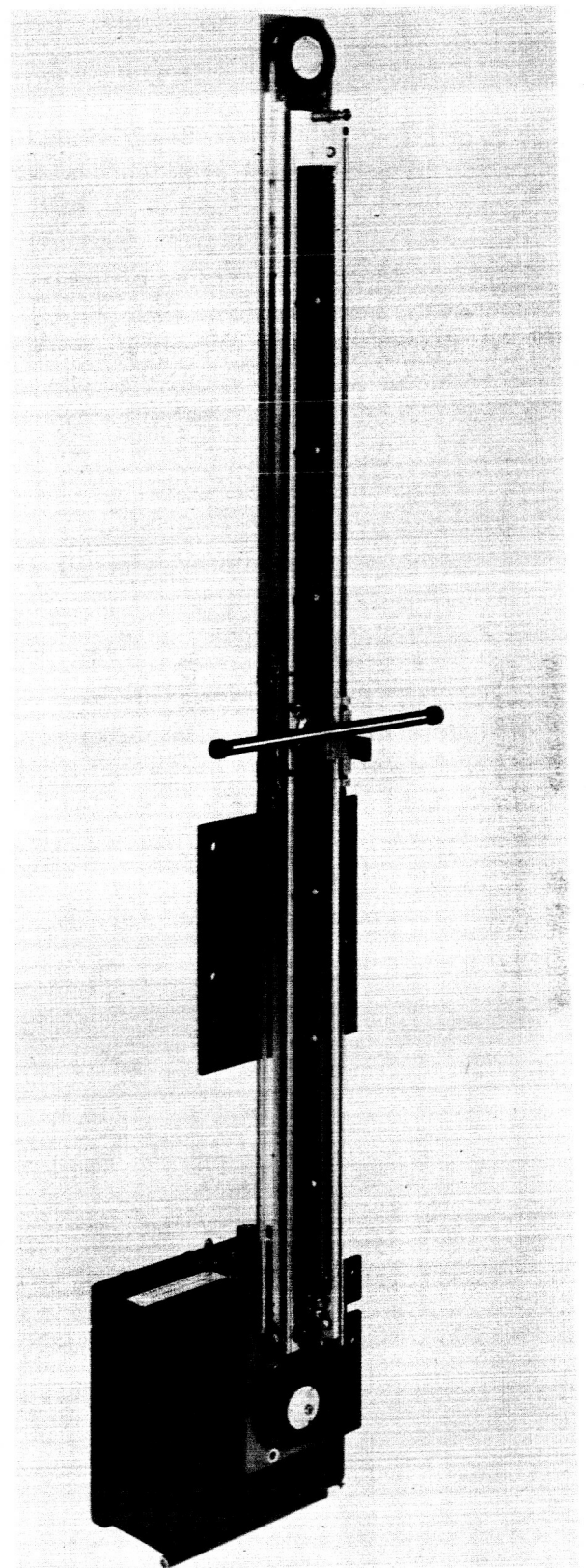
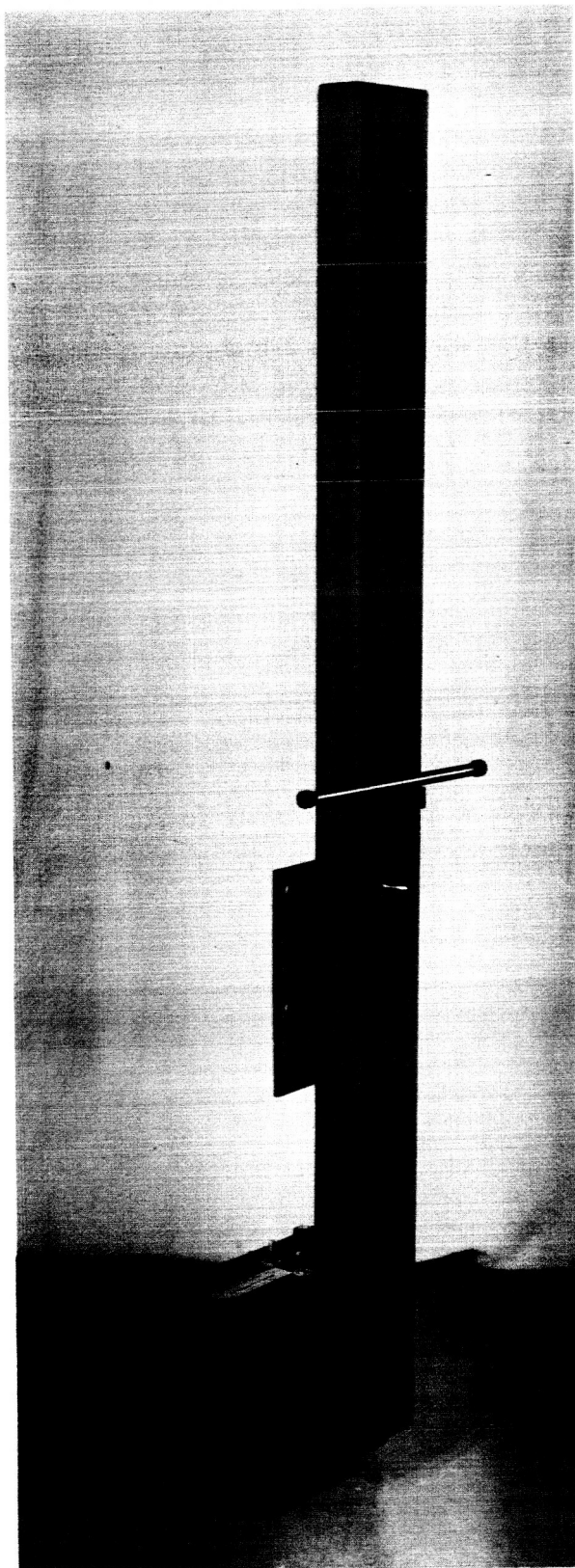


Figure C3

The Linear Displacement Target used for the  $\tau_y$  response measures of this study shown with (left) and without (right) the protective housing for the linear slide-wire potentiometer.

The luminous target rod, identical to that used with the angular position target, was attached directly to the driven slide-wire contact arm. The outside arms of the center-tapped slide-wire potentiometer were connected to a dual voltage regulated DC power supply with the center-top of the slide wire returned to the common terminal of the power supply. A digital voltmeter connected to the movable contact arm-target assembly provided a measure of the displacement of the target above or below the center-tap position of the slide wire. The output voltages of the dual power supply, normally 30 volts, were separately adjusted so that a 2 volts per 1 inch calibration scale factor could be established where polarity reversals of the output signal indicated target elevation or depression below its electrical mid-point. Subject or experimenter control of the target motions was provided by circuitry similar to that used for control of the angular position target.

The Dual Axis Target assembly used for the  $\tau_y$  and  $\tau_z$  subjective estimates of the visual dead ahead position utilized the writing element of a commercial X - Y type curve follower recorder (Houston Instrument Corporation, Model HR-101) to provide two-dimensional motions of the visual target. The writing element, enclosed in a custom fabricated housing, was fixed to the instrument shelf component of the variable attitude chair directly in front of the subject at eye level. The 11 inch x 17 inch writing surface was oriented such that the long dimension was directed vertically (see Figure C 4). A 1 inch x 1 inch luminous target cross fixed to the writing stylus of the

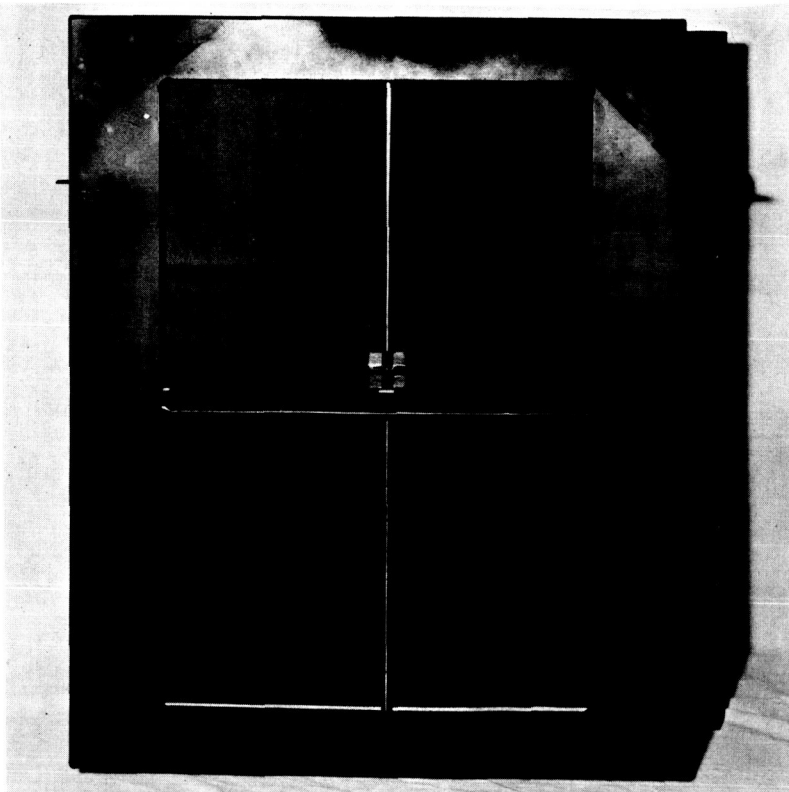


Figure C4

The Dual-Axis Target used for the  $\tau_y$  and  $\tau_z$  response measures of this study.

recorder could be made to move in the horizontal direction along a supporting carriage arm or in the vertical direction when the entire carriage arm was displaced. With this recorder, each form of motion was controlled by a null-seeking servomechanism operated in the position mode where the displacements of the writing stylus-target cross were directly proportional to the magnitude and polarity of DC voltage command signals fed to the X and Y input amplifiers.

The command signal for the X amplifier was derived from a hand controller utilizing a multi-turn rotary potentiometer which was energized from a floating-output, voltage regulated, DC power supply. A separate low-impedance potentiometer was shunted across the power supply with its contact arm returned to circuit ground. This potentiometer, located in the Monitor Console, allowed the experimenter to program random target offsets between subjective estimates without changing the sensitivity scale factor of the hand controller potentiometer. Identical controller and offset circuitry were provided for the Y amplifier channel. The exact position of the target following each subjective judgment task was recorded by a digital readout voltmeter that was sequentially switched from the input of the X amplifier channel to the Y amplifier channel to obtain a direct measure of the DC command signals effecting the target displacements.

A photograph of the Monitor Console used to house the experimenter related elements of the various target assemblies is presented in Figure C5 where it is shown installed in its actual operating position aboard the Pensacola Centrifuge. As viewed from top to bottom, the sloped front of the console housed a master power distribution panel for central control of the entire target instrumentation system; a control panel for experimenter operation of the Digital Angular Position Target which included the four digit decimal readout indicator; the digital voltmeter used to record the position of either the Dual-Axis Target or Linear Displacement Target; and a control panel for experimenter operation of the latter target assembly. Various target power supplies and audio communications equipments may be seen installed in the console area beneath the projecting writing desk.



Figure C5

Photograph of the Monitor Console installed aboard the centrifuge.

Unclassified

Security Classification

DOCUMENT CONTROL DATA - R&D		
<i>(Security classification of title, body of abstract and indexing annotation must be entered when the overall report is classified)</i>		
1. ORIGINATING ACTIVITY <i>(Corporate author)</i> U. S. Naval Aerospace Medical Institute Pensacola, Florida		2a. REPORT SECURITY CLASSIFICATION <b>UNCLASSIFIED</b>
		2b. GROUP
3. REPORT TITLE Otolith Shear and the Visual Perception of Force Direction: Discrepancies and a Proposed Resolution		
4. DESCRIPTIVE NOTES <i>(Type of report and inclusive dates)</i>		
5. AUTHOR(S) <i>(Last name, first name, initial)</i> Correia, Manning J., Hixson, W. Carroll, and Niven, Jorma I.		
6. REPORT DATE 1 December 1965	7a. TOTAL NO. OF PAGES 73	7b. NO. OF REFS 11
8a. CONTRACT OR GRANT NO. NASA R-93	9a. ORIGINATOR'S REPORT NUMBER(S) NAMI-951	
b. PROJECT NO. MR005.13-6001		
c.	9b. OTHER REPORT NO(S) <i>(Any other numbers that may be assigned this report)</i>	
d.	126	
10. AVAILABILITY/LIMITATION NOTICES Qualified requesters may obtain copies of this report from DDC. Available, for sale to the public, from Federal Clearinghouse for Scientific and Technical Information, Springfield, Virginia.		
11. SUPPLEMENTARY NOTES		12. SPONSORING MILITARY ACTIVITY
13. ABSTRACT  Judgments of subjective vertical and horizon were obtained during exposure to five angular directions and five magnitudes of linear acceleration stimuli varied independently on a human centrifuge. The visual perception of the orientation of the force field could not be shown to be a linear function of the otolith shear-directed component, and discontinuities in response for identical stimuli were observed. A tangent equation expression which resolves these discrepancies and better predicts the subjective response is proposed. A rationale for this equation and generalizations relative to extraterrestrial environments are discussed.		



14. KEY WORDS	LINK A		LINK B		LINK C	
	ROLE	WT	ROLE	WT	ROLE	WT
Linear accelerations						
Subjective vertical						
Subjective horizon						
Otolith shear						
Visual perception						

## INSTRUCTIONS

1. **ORIGINATING ACTIVITY:** Enter the name and address of the contractor, subcontractor, grantee, Department of Defense activity or other organization (*corporate author*) issuing the report.

2a. **REPORT SECURITY CLASSIFICATION:** Enter the overall security classification of the report. Indicate whether "Restricted Data" is included. Marking is to be in accordance with appropriate security regulations.

2b. **GROUP:** Automatic downgrading is specified in DoD Directive 5200.10 and Armed Forces Industrial Manual. Enter the group number. Also, when applicable, show that optional markings have been used for Group 3 and Group 4 as authorized.

3. **REPORT TITLE:** Enter the complete report title in all capital letters. Titles in all cases should be unclassified. If a meaningful title cannot be selected without classification, show title classification in all capitals in parenthesis immediately following the title.

4. **DESCRIPTIVE NOTES:** If appropriate, enter the type of report, e.g., interim, progress, summary, annual, or final. Give the inclusive dates when a specific reporting period is covered.

5. **AUTHOR(S):** Enter the name(s) of author(s) as shown on or in the report. Enter last name, first name, middle initial. If military, show rank and branch of service. The name of the principal author is an absolute minimum requirement.

6. **REPORT DATE:** Enter the date of the report as day, month, year, or month, year. If more than one date appears on the report, use date of publication.

7a. **TOTAL NUMBER OF PAGES:** The total page count should follow normal pagination procedures, i.e., enter the number of pages containing information.

7b. **NUMBER OF REFERENCES:** Enter the total number of references cited in the report.

8a. **CONTRACT OR GRANT NUMBER:** If appropriate, enter the applicable number of the contract or grant under which the report was written.

8b, 8c, & 8d. **PROJECT NUMBER:** Enter the appropriate military department identification, such as project number, subproject number, system numbers, task number, etc.

9a. **ORIGINATOR'S REPORT NUMBER(S):** Enter the official report number by which the document will be identified and controlled by the originating activity. This number must be unique to this report.

9b. **OTHER REPORT NUMBER(S):** If the report has been assigned any other report numbers (*either by the originator or by the sponsor*), also enter this number(s).

10. **AVAILABILITY/LIMITATION NOTICES:** Enter any limitations on further dissemination of the report, other than those

imposed by security classification, using standard statements such as:

- (1) "Qualified requesters may obtain copies of this report from DDC."
- (2) "Foreign announcement and dissemination of this report by DDC is not authorized."
- (3) "U. S. Government agencies may obtain copies of this report directly from DDC. Other qualified DDC users shall request through \_\_\_\_\_."
- (4) "U. S. military agencies may obtain copies of this report directly from DDC. Other qualified users shall request through \_\_\_\_\_."
- (5) "All distribution of this report is controlled. Qualified DDC users shall request through \_\_\_\_\_."

If the report has been furnished to the Office of Technical Services, Department of Commerce, for sale to the public, indicate this fact and enter the price, if known.

11. **SUPPLEMENTARY NOTES:** Use for additional explanatory notes.

12. **SPONSORING MILITARY ACTIVITY:** Enter the name of the departmental project office or laboratory sponsoring (*paying for*) the research and development. Include address.

13. **ABSTRACT:** Enter an abstract giving a brief and factual summary of the document indicative of the report, even though it may also appear elsewhere in the body of the technical report. If additional space is required, a continuation sheet shall be attached.

It is highly desirable that the abstract of classified reports be unclassified. Each paragraph of the abstract shall end with an indication of the military security classification of the information in the paragraph, represented as (TS), (S), (C), or (U).

There is no limitation on the length of the abstract. However, the suggested length is from 150 to 225 words.

14. **KEY WORDS:** Key words are technically meaningful terms or short phrases that characterize a report and may be used as index entries for cataloging the report. Key words must be selected so that no security classification is required. Identifiers, such as equipment model designation, trade name, military project code name, geographic location, may be used as key words but will be followed by an indication of technical context. The assignment of links, roles, and weights is optional.